ChemComm

FEATURE ARTICLE

View Article Online
View Journal | View Issue

Cite this: *Chem. Commun.*, 2023, **59**, 7004

Redox-neutral carbon–heteroatom bond formation under photoredox catalysis†

Sumit Ghosh, ‡[a] Souvik Majumder, ‡[a] Debashis Ghosh ‡[b] and Alakananda Hajra *[a]

Received 17th April 2023,
Accepted 4th May 2023

DOI: 10.1039/d3cc01873c

rsc.li/chemcomm

Recently, visible-light-mediated photoredox catalysis has been emerging as one of the fastest growing fields in organic chemistry because of its low cost, easy availability and environmental benignness. In the past five years, a new yet challenging trend, visible-light-induced redox-neutral carbon–heteroatom bond formation reaction involving presumed radical intermediates, has been flourishing rapidly. Although mostly transition metal-based photoredox catalysts were reported, a few organophotoredox catalysts have also shown efficacy towards carbon–heteroatom bond formation reactions. This review intends to summarize the recent research progress in redox-neutral carbon–heteroatom bond formations based on active intermediate(s) involved under photoredox catalysis.

1. Introduction

The metamorphic nature of organic synthesis has broadened the application towards biochemistry, materials sciences and pharmaceutical industries.[1] Therefore, the focus is shifting quickly toward visible-light-mediated chemical reactions,[2] which circumvent the harshness of reagents and use of high-energy UV light.[3] On the other hand, carbon–heteroatom bonds were found to be in several biologically active molecules (Fig. 1).[4] Among the various carbon–heteroatom bond formation methodologies,[5] a redox-neutral protocol is achieving tremendous interest nowadays.[6] A redox-neutral reaction is a type of redox reaction that occurs within the reaction system without employing any species present solely to oxidize or reduce the photocatalyst.[7] Therefore, the use of stoichiometric amounts of environmentally unfriendly oxidants and/or reductants is completely avoided by this method. Moreover, harvesting visible-light in redox-neutral carbon–heteroatom bond formation can be more interesting (Fig. 2). To date, various review articles, including one on redox-neutral radical C–C cross-coupling, have summed up the recent progress in visible-light photocatalysis;[8] however, no recent review exists on the photo-induced redox-neutral carbon–heteroatom bond formation reactions. Recently, extensive research has been done in this regard using metallaphotoredox as well as

[a] *Department of Chemistry, Visva-Bharati (A Central University), Santiniketan 731235, India. E-mail: alakananda.hajra@visva-bharati.ac.in*
[b] *Department of Chemistry, St. Joseph's University, Bangalore 560027, Karnataka, India*

† This review article is dedicated to Professor Shigeru Yamago on the occasion of his 60th birthday.
‡ These authors have equal contributions and first authorship.

Sumit Ghosh

Sumit Ghosh completed his BSc from Burdwan University in 2014. He achieved his MSc from IIT Kanpur in 2016. Recently, he has been working with Dr Alakananda Hajra in Visva-Bharati University. He is enlisted in the Stanford University's single year top 2% scientists of the world in 2022. His research interest is functionalizations of different heterocycles.

Souvik Majumder

Souvik Majumder completed his bachelors from Bidhannagar College under West Bengal State University in the year 2019. He completed his MSc at Visva-Bharati University in 2021. Currently, he has started working with Dr Alakananda Hajra at Visva-Bharati University. The focus of his research is on metal-catalyzed C–H activation and functionalizations.

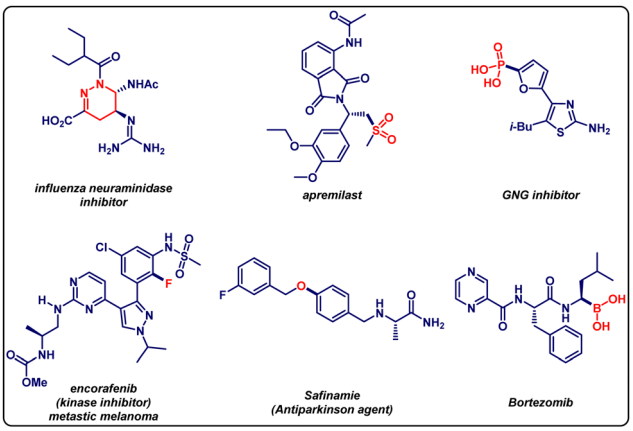

Fig. 1 Some examples of drugs containing carbon–heteroatom bonds.

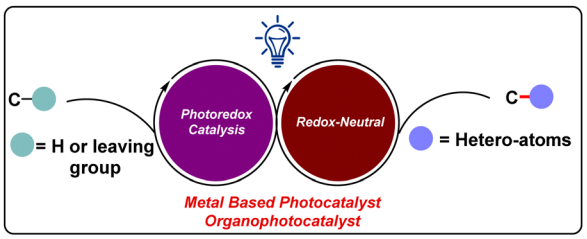

Fig. 2 Visible-light-induced redox-neutral carbon–heteroatom formation.

organo-photoredox catalysts (Fig. 3). Among metal-based photoredox catalysts, mostly late transition-metals (*e.g.*, Ru, Ir *etc.*) have been reported. Although, a few first row transition-metal-based organometallic complexes have been reported as supporting catalysts in combination with a photo-redox catalyst, which is either a late transition-metal-based or organo-photoredox catalyst. The reported organophotoredox catalysts include Rose Bengal, 1,2,3,5-tetrakis(carbazole-9-yl)-4,6-dicyanobenzene (4-CzIPN), 2,4,6-tris(diphenylamino)-5-fluoroisophthalonitrile (3DPAFIPN), diphenyldibenzocarbazole (CBZ6) *etc.*

A general mechanistic scheme for light-mediated redox-neutral carbon–heteroatom coupling using photoredox catalysts is represented in Scheme 1. Depending on the redox potential of the excited state of the photocatalyst (**PC**), either oxidative quenching (step I) with electron acceptors (alkyl halides, aryl imines, aryl diazonium salt, *N*-Ts-protected 1-aminopyridinium salt, NHPI, dimethylsulfamoyl chloride, Selectfluor®, *N*-hydroxyphthalimide ester, high-valent metal complexes, *etc.*) or reductive quenching (step II) with electron donors (amines, carboxylates, alkenes, hydrazones anions, halides *etc.*) can initiate the photoredox-mediated catalytic cycle. In some cases, the combination of an additional catalytic cycle (organocatalysis or transition-metal catalysis) with photoredox catalysis is essential for a successful coupling. Subsequently, the oxidized or reduced photocatalyst can oxidize (step III, Scheme 1) or reduce (step IV, Scheme 1) a reactant in the ground state redox reaction and follow-up reactions will lead to carbon–heteroatom (C–X) bond formation.[9]

In this scenario, we have significantly contributed to visible-light-induced carbon–hetero atom bond formation using photoredox catalysts for more than 5 years.[9,10] In continuation of our work on these carbon–heteroatom bond formation reactions and photochemistry, we wish to report, herein, a recent update on visible-light-induced redox-neutral C–X bond

Debashis Ghosh

Dr Debashis Ghosh has received his PhD from CSIR-Central Salt and Marine Chemicals Research Institute, Bhavnagar, India, with a thesis on the development of chiral catalysis for asymmetric allylation reaction under the supervision of Dr Sayed H. R. Abdi in 2015. He worked in Prof. Koji Tanaka's research group at Kyoto University in the field of electrochemistry, 2015–2018. Thereafter, he worked in Prof. Osamu Ishitani's research group at Tokyo Institute of Technology, in the field of photochemistry, 2018–2019. Presently, he is an assistant professor at St. Joseph's University, Bengaluru, India. His current research interest includes CO_2 reduction chemistry, asymmetric catalysis and functionalization of heterocycles.

Alakananda Hajra

Dr Alakananda Hajra did a PhD under the supervision of Prof. B. C. Ranu from Indian Association for the Cultivation of Science (IACS), Kolkata in 2002 and then joined SUNY at Albany, USA as a postdoctoral research fellow in Prof. Frank M. Hauser's group (2002–2004). He was also a JSPS research fellow in the University of Tokyo and worked with Prof. Eiichi Nakamura and Prof. Masaharu Nakamura from November 2004 to May 2006 and then he joined Visva-Bharati University. He also worked with Prof. N. Yoshikai, NTU, Singapore for one year (2011–2012). He has been awarded the Prof. D. K. Banerjee Memorial Lecture Award for the year 2015 from the Indian Institute of Science, Chemical Research Society of India (CRSI) Bronze Medal Award for the year 2018, and Professor D. Nasipuri Memorial Award for the year 2019 by Indian Chemical Society. His research interests include the development of new synthetic methodologies and green synthetic procedures.

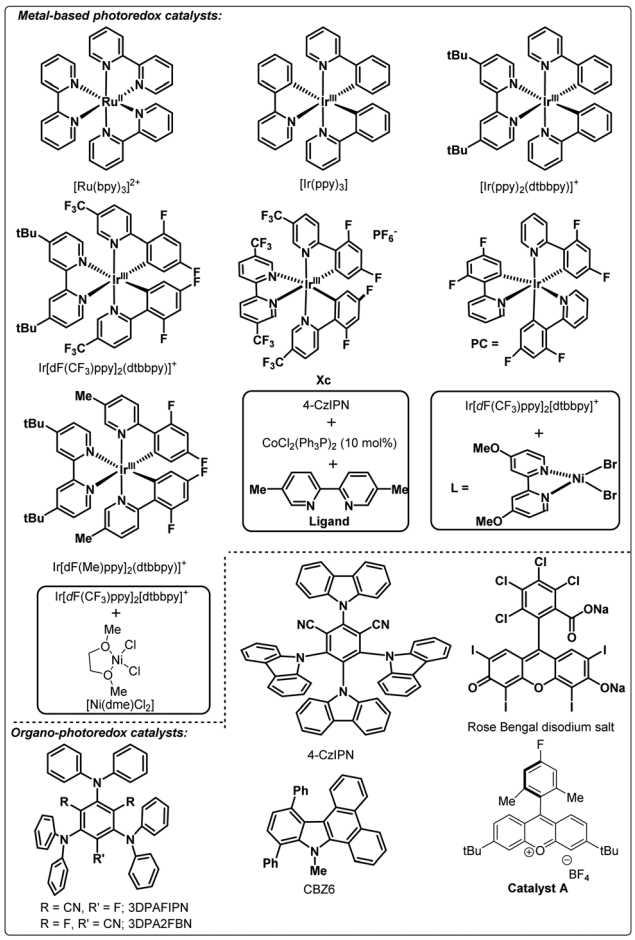

Fig. 3 Metal-based and metal-free photoredox catalysts reported for redox-neutral carbon–heteroatom bond formation reactions.

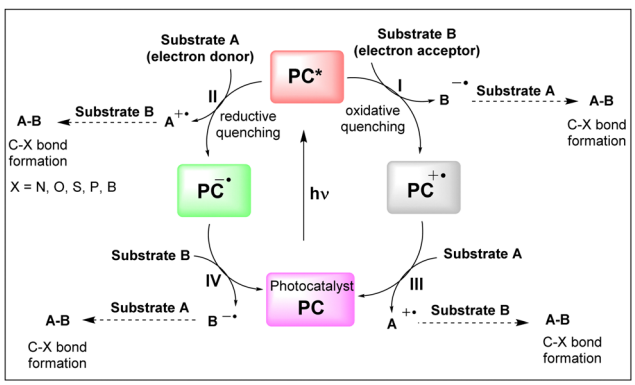

Scheme 1 General mechanistic considerations for light-mediated redox-neutral carbon–heteroatom bond formation reactions.

formation reactions using photoredox catalysts up until March, 2023. Due to the involvement of various types of radical intermediates, we thought of classifying these C–X bond formation reactions into (i) heteroatom-centered radical reactions, (ii) carbon-centered radical reactions, (iii) mixed carbon- and heteroatom-centered radical reactions, (iv) carbene intermediate-assisted reactions, and (v) combination of photocatalysts with other metal catalysts: metallaphotoredox catalysts.

2. Heteroatom-centered radical reactions

It is well established in the literature that various photo-induced redox-neutral carbon–heteroatom bond formation reactions proceed *via* the formation of a heteroatom-centered radical at the initial stage of the photoredox cycle. In this section, we will present chronologically the examples of C–X bond formation reactions involving this kind of active intermediate.

In 2014, Knowles and co-workers[11] demonstrated a novel visible-light photoredox protocol for the intramolecular hydroamination of aryl olefins to form a direct C–N bond. The main advantage of the method is it being a rare example of the use of aminium radical cations derived from simple amine precursors in catalytic C–N bond formation. The hydroamination of aryl olefins **2a** used $Ir(ppy)_2(dtbbpy)PF_6$ as a photocatalyst (PC) under blue LED light irradiation. The reactions underwent efficiently to give the desired product **2b** with up to 95% yield at room temperature (Scheme 2). The reaction showed good functional group tolerance and a broad substrate scope for both the aryl rings. Moreover, heterocyclic olefin acceptors such as pyridine, thiophene, and furan-containing substrates underwent cyclization without difficulties and some fused bicyclic systems were also synthesized through this methodology. Mechanistically, the aryl olefin underwent one-electron oxidation with the Ir-photocatalyst to generate aminium radical cation **2i**, which then subsequently participated in a C–N bond formation reaction to produce radical **2ii**. Thereafter, one-electron reduction of intermediate **2ii** afforded the carbanion **2iii** and finally, proton transfer offered the desired hydroamination product **2b** (Scheme 2).

In 2017, Studer's group[12] reported a visible-light-mediated decarboxylation of α-imino-oxy propionic acids **3a** for the formation of iminyl radicals in the presence of $Ir(dFCF_3ppy)_2(dtbbpy)PF_6$ as a photoredox catalyst and coupled with electron-deficient alkenes **3b**. The reaction proceeded through *N*-radical generation, iminyl radical cyclization, intermolecular conjugate addition to a Michael acceptor, and single-electron reduction, which led to the formation of various pyrroline derivatives **3c** (Scheme 3). Interestingly, it was an overall redox-neutral process. CsF was found to be the best choice as a base and without a base, the reaction did not proceed. Under the optimized reaction conditions, α,β-unsaturated ketones, esters, amides and a phosphonate as a radical acceptor worked very well, affording good to excellent yields, whereas phenyl vinyl sulfone as an acceptor provided a lower yield. The method showed good tolerance of both electron-rich and electron-poor substitutions on the phenyl rings resulting in the desired pyrroline derivatives in good yields. Based on the mechanistic study, at first, visible-light-promoted photoexcitation of $Ir^{III}(dFCF_3ppy)_2(dtbbpy)PF_6$ gave the excited $^*Ir^{III}(dFCF_3ppy)_2(dtbbpy)PF_6$ complex. It then underwent SET with carboxylate **3i**, generated from deprotonation

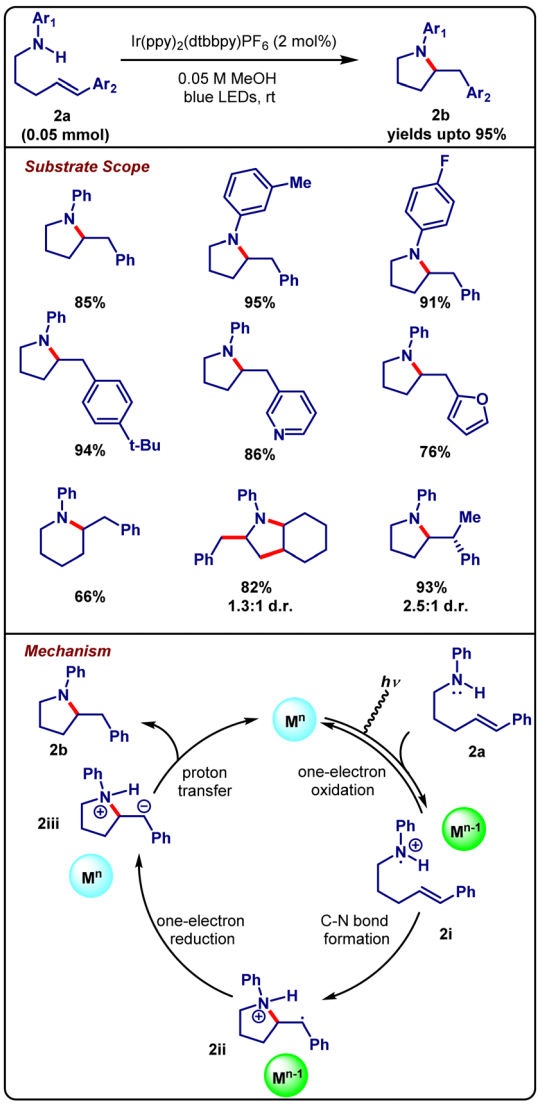

Scheme 2 Photoredox-catalyzed intramolecular hydroamination of aryl olefins (Knowles method).

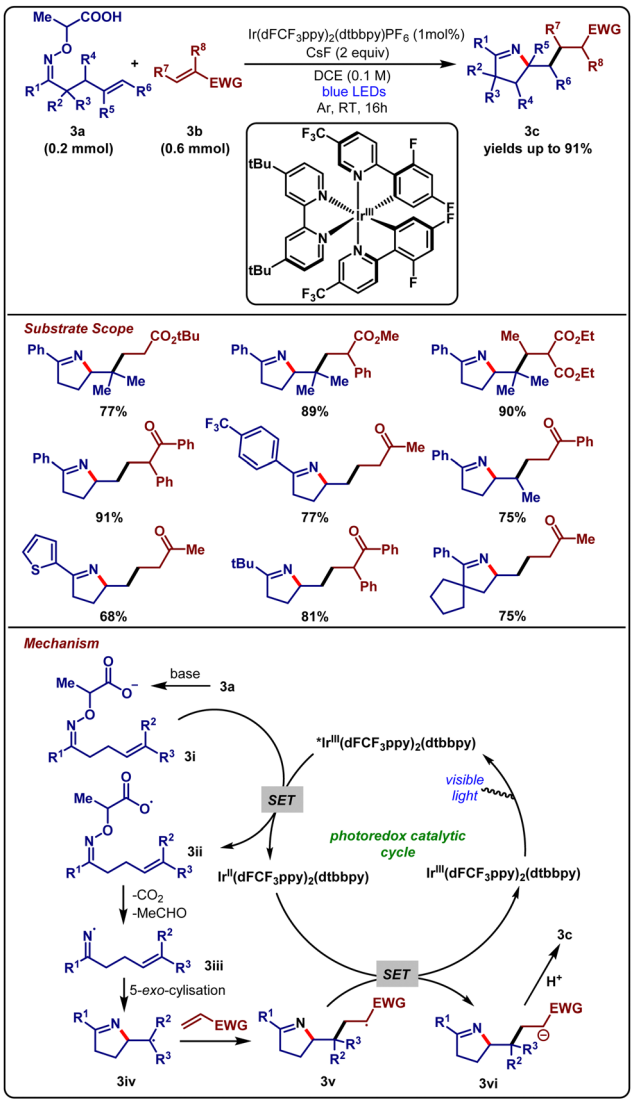

Scheme 3 Photoredox-catalyzed decarboxylation of α-imino-oxy propionic acids (Studer method).

of substrate **3a**, forming carboxy radical **3ii**. Then, subsequent removal of CO_2 and acetaldehyde from **3ii** generated iminyl radical **3iii**. Afterward, 5-*exo*-cyclization of **3iii** afforded C-centred radical **3iv**, which reacted by an intermolecular conjugate addition with alkene **3b** to produce the corresponding electrophilic adduct radical **3v**. The overall photoredox cycle ended up with SET reduction of **3v** by $Ir^{II}(dFCF_3ppy)_2(dtbbpy)PF_6$ to provide **3vi** and regenerated the ground state photocatalyst $Ir^{III}(dFCF_3ppy)_2(dtbbpy)PF_6$. Finally, protonation of **3vi** led to the formation of pyrroline **3c**.

In 2019, Cheng *et al.*[13] devised a visible-light-promoted photoredox-catalyzed sulfonamidation of enol acetates **4a** using *N*-arylsulfonyl-1-aminopyridine salts **4b** to synthesize a bunch of α-amino ketones **4c** upon irradiation with a blue LED in the presence of photocatalyst $Ir(ppy)_3$ (Scheme 4). This methodology is useful for C–N bond formation under redox-neutral photocatalysis and mild reaction conditions, and does not require any external oxidant. Acetonitrile was used as the most efficient solvent for the reaction. While exploring the substrate scope of the reaction, it was found that the reaction was successful for various substrates containing electron-rich arenes. However, phenyl-, naphthyl- and 2-thiophenyl-substituted enol acetates are prerequisites for the reaction because alkyl-substituted amino ketone synthesis was unsuccessful. Moreover, *N*-arylsulfonyl-1-aminopyridine salts bearing both electron-donating as well as moderately electron-deficient substituents produced the corresponding amino ketone in good yields. However, more strongly electron-withdrawing groups like *para*-CF_3 and *para*-NO_2 did not participate in this coupling reaction.

According to the literature reports, a mechanism has been proposed by the authors and is sketched in Scheme 4. At first, the blue LED light excited the photocatalyst $Ir(ppy)_3$ and generated excited $^*Ir(ppy)_3$, which reduced *N*-Ts-protected 1-aminopyridinium salt **4b** to *N*-centered radical **4i** *via* the

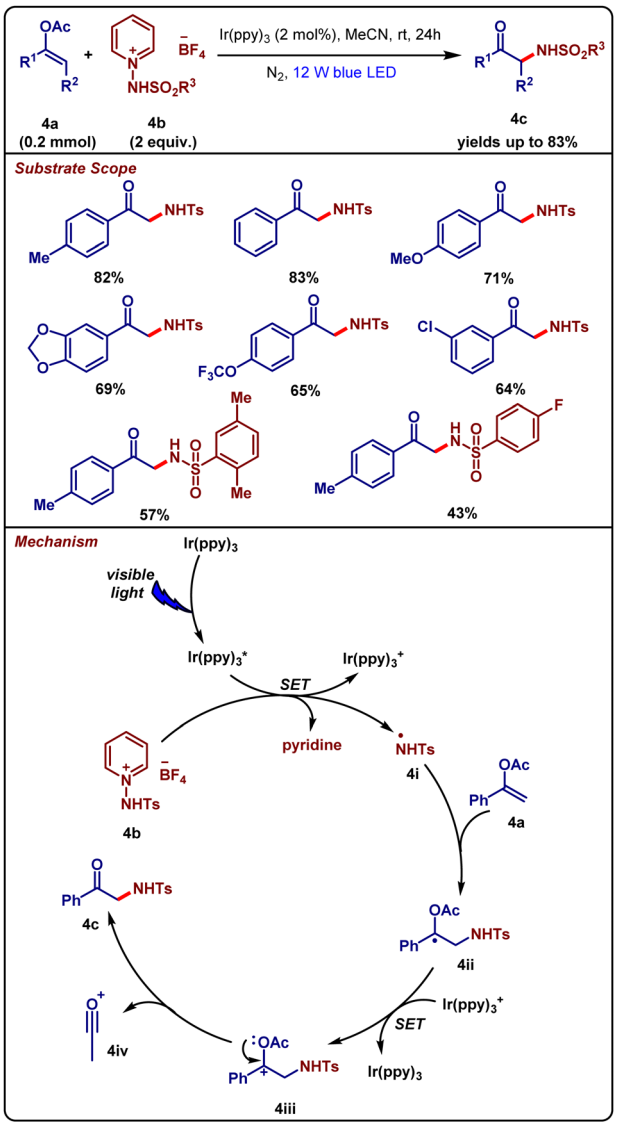

Scheme 4 Photoredox-catalyzed sulfonamidation of enol acetates to α-amino ketones (Cheng method).

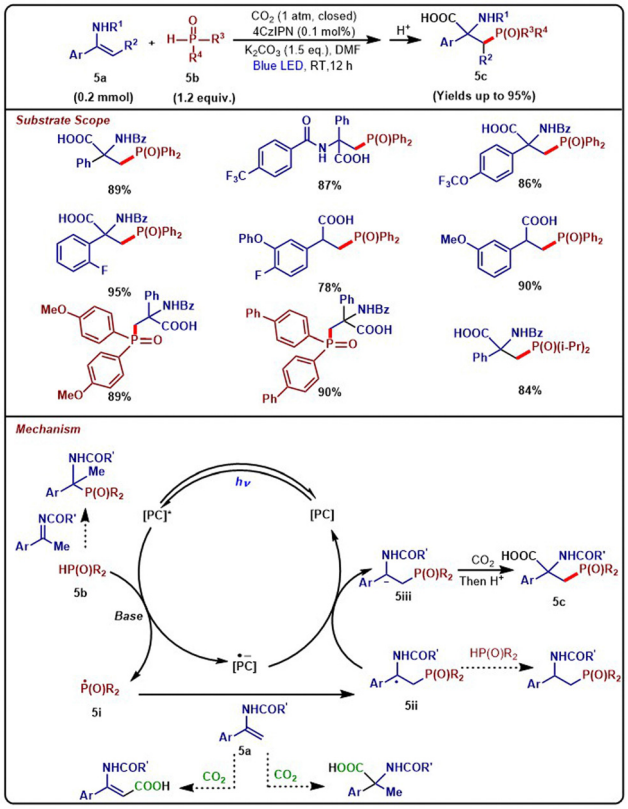

Scheme 5 Photoredox-catalyzed phosphonocarboxylation of alkenes (Yu method).

SET process and self-oxidation gave $[Ir(ppy)_3]^+$. Next, *N*-centred radical **4i** reacted with the enol double bond of **4a** to give radical intermediate **4ii** and subsequent oxidation by $[Ir(ppy)_3]^+$ generated cation **4iii** along with regeneration of $Ir(ppy)_3$ for the next catalytic cycle. Finally, the elimination of acetyl cation **4iv** from **4iii** furnished the resulting amino ketone **4c**.

In the same year (2019), Yu *et al.*[14] devised catalytic redox-neutral phosphonocarboxylation of alkenes **5a** with H–P(O) compounds **5b** at room temperature conditions. β-Phosphono α-amino acids **5c** were achieved in good to excellent yields using this protocol within 12 h (Scheme 5). The authors examined different photocatalysts, such as $Ru(bpy)_3Cl_2$, $Ir[(ppy)_2(dtbpy)]PF_6$ and 4CzIPN, but 4CzIPN was found to be the most suitable PC for this reaction system. The enamides containing electron-donating and electron-withdrawing groups, as well as heteroarenes reacted smoothly under the optimized reaction conditions. The alkyl enamide produced the hydrophosphinylation product instead of the desired decarboxylative product. Along with that, the authors also explored the scope of H–P(O) compounds. In addition, the authors performed mechanistic studies, including radical trapping with TEMPO, radical clock tests and isotope levelling with D_2O. Based on these supporting experiments, a plausible catalytic cycle was proposed as sketched in Scheme 5. The reaction was initiated with the generation of phosphonyl radical **5i** from H–P(O) compound **5b** *via* single-electron-transfer (SET) in the presence of the excited photocatalyst and a base. Thereafter, radical **5i** was added to the C=C double bonds of enamides **5a** to generate α-amido radical **5ii**. Intermediate **5ii** subsequently underwent SET in the presence of the reduced photocatalyst and generated α-amido carbanion **5iii**, which further reacted with CO_2 to afford the desired product β-phosphono α-amino acid **5c**. As it was shown in the above scheme, there were several by-products formed along with the main product **5c**.

In 2021, Liu and co-workers[15] devised alkene aminoarylation *via* a photoredox-neutral protocol. The optimal catalytic system comprising $Ru(bpy)_3Cl_2$ as the photocatalyst, $^tBuCO_2K$ as the base and DCE as the solvent allowed for intramolecular aminoarylation of hydrazone **6a**. A series of N-heterocyclic products, 1,4,5,6-tetrahydropyridazines **6b**, were achieved with up to 92% yield *via* a cascade of hydrazonyl radical cyclization and Smiles–Truce aryl transfer. The methodology showed excellent functional group tolerance, including halogen, methoxy and trifluoromethyl substituents. Based on the previous

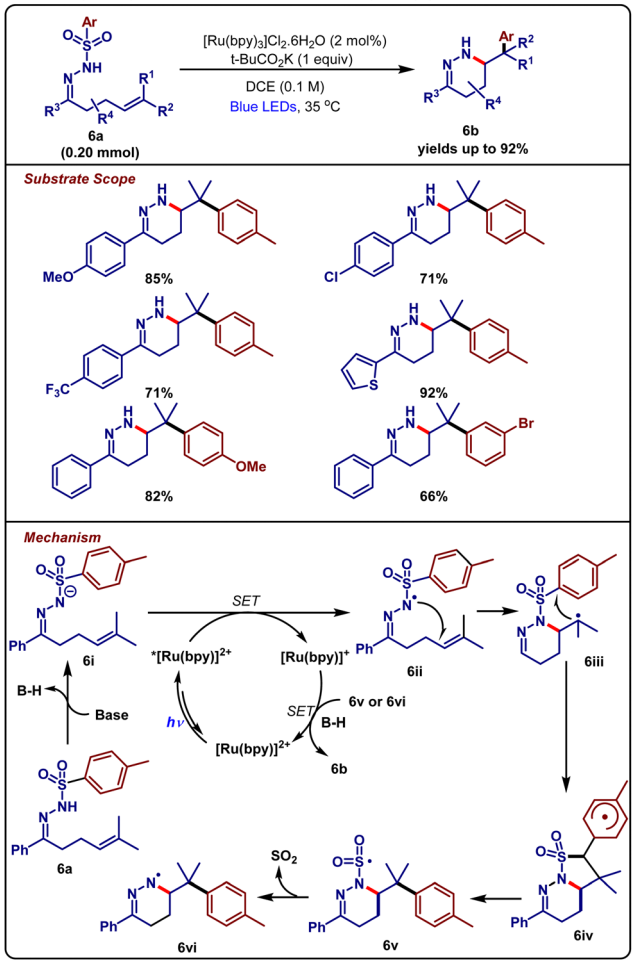

Scheme 6 Photoredox-catalyzed alkene aminoarylation (Liu method).

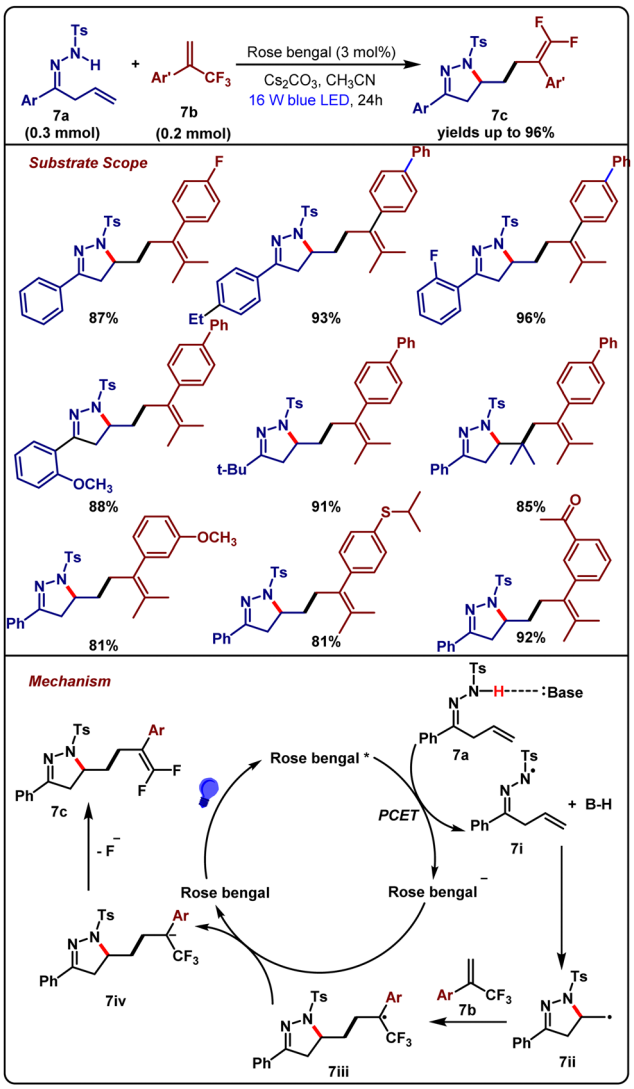

Scheme 7 Photoredox-catalyzed tandem radical cyclization/defluorinated alkylation of β,γ-unsaturated hydrazones and α-trifluoromethyl alkenes (Zhou method).

literature reports and fluorescence quenching experiments, the authors proposed a plausible mechanism, as shown in Scheme 6. The catalytic cycle was commenced by the deprotonation of hydrazone **6a** under basic conditions providing the anionic intermediate **6i**. Subsequently, *N*-centred radical **6ii** was formed *via* SET oxidation by excited photocatalyst $*[Ru(bpy)_3]^{2+}$. Thereafter, 6-*exo*-*trig* cyclization of electrophilic radical **6ii** afforded alkyl radical **6iii**. Then, the regioselective radical cyclization of intermediate **6iii** on the *ipso*-position of the sulfonylaryl moiety generated intermediate **6iv**. The regeneration of aromaticity of **6iv** *via* homolytic fragmentation of the C_{Ar}–S bond led to sulfonyl radical **6v**. Finally, the extrusion of SO_2 from the sulfonyl radical followed by the oxidation of reduced photosensitizer Ru-complex to complete the catalytic cycle furnished the desired product **6c**.

Among the various fluorine-containing compounds, *gem*-difluoroalkenes are specified as a class of unique fluorinated motifs having several agrochemical, medicinal and organic chemistry applications.[16] In 2021, Sun, Yu and Zhou *et al.*[17] established an efficient visible-light-mediated *N*-radical-promoted tandem radical cyclization/defluorinated alkylation of β,γ-unsaturated hydrazones **7a** with α-trifluoromethyl alkenes **7b** in the presence of Rose Bengal as a photocatalyst to synthesise a bunch of dihydropyrazole-fused *gem*-difluoroalkene products with up to 96% yield within 24 h (Scheme 7). The prescribed methodology is useful for the formation of C–N bonds under redox-neutral, metal-free, and mild conditions. The Stern–Volmer quenching studies indicated that the Cs_2CO_3 quenched with the excited Rose Bengal, which proved that N–H bond activation was promoted by a proton-coupled electron transfer process. The reaction showed a broad range of functional group tolerance. Therefore, hydrazones possessing electron-donating as well as electron-withdrawing groups on the phenyl rings produced the desired products in excellent yields. Similarly, substitutions on α-trifluoromethyl alkenes also gave the *gem*-difluoroalkene in good yields under the optimized reaction conditions. Based on the literature precedents and experimental studies, the authors proposed a plausible mechanistic pathway for the reaction, as depicted in Scheme 7. In the beginning, visible-light irradiation generated excited-state Rose

Bengal*, which oxidized **7a** with the help of base to create *N*-center hydrazonyl radical **7i**. Then, the radical **7i** reacted with the internal olefin to give C-center radical **7ii**, which subsequently interacted with α-trifluoromethyl alkene **7b** to form the intermediate **7iii**. After that, Rose Bengal reduced the radical **7iii** to anion **7iv** *via* a single-electron transfer process. Finally, the removal of F^- from **7iv** afforded the desired final product **7c**.

In the same year (2021), Wang, Li and Wang *et al.*[18] disclosed a selective sulfonamidation and sulfonation methodology *via* visible-light-catalyzed tandem cyclization of electron-deficient alkenes **8a** with sulfamoyl and sulfonate radicals from readily accessible dimethylsulfamoyl chloride **8b**. This protocol comprised high efficiency, and external oxidant-free and mild conditions making it more facile towards the later stages of functionalization for complex molecules. Initially, the desired product **8d** was obtained with a 92% yield using Ir{dF(CF$_3$)ppy}$_2$(dtbbpy)PF$_6$ as the photocatalyst, Na_2CO_3 as the base and MeCN as the solvent under irradiation with blue LEDs (25 W) at room temperature (Scheme 8). It was also observed that by modifying the iridium catalysts such as Ir(btp)$_2$(*t*-Leu), Ir(btp)$_2$Ala, and Ir(btp)$_2$Leu, with 2-(2-pyridyl)benzothiophene and various amino acids as ligands exclusively afforded product **8d;** however lower yields were achieved. Under the optimized reaction conditions, a diverse range of aromatic amines bearing electron-donating groups afforded the desired sulfonate products in good yields. But sluggishness was observed in the case of amines containing electron-withdrawing groups at the *para*-position, which suggested that the reaction was an electrophilic cyclization process. To establish the reaction mechanism, the authors have performed the radical trapping experiment using TEMPO, which produced the radical trapped products confirming a radical mechanism. Moreover, they observed that dimethylaminosulfonyl chloride was able to generate the dichlorinated isomers as dimethylaminosulfanedione and *N*-methyl *N*-sulfonylmethanaminium under basic conditions, which suggested that sulfamoyl radicals were directly generated from dimethylaminosulfonyl chloride. Based on the previous literature reports and the control experiments, the authors proposed the reaction mechanism as depicted in Scheme 8. Initially, the precatalyst, Ir^{III} was excited by blue LEDs to $*Ir^{III}$, which reduced dimethylaminosulfonyl chloride **8b** to give the sulfomyl radical. Next, the dechlorination gave intermediate **8i** under alkaline conditions, which then simultaneously released dimethyl amine and sulfonate radicals under the action of the hydroxyl and $*Ir^{III}$ photocatalyst. Then, SO_3^- radical **8i** added to the carbon–carbon double bond of **8a**, producing radical **8ii**, which underwent intramolecular cyclization to generate cyclic radical intermediate **8iii**. The SET oxidation of intermediate **8iii** provided the corresponding cation **8iv** with the regeneration of Ir^{III} from Ir^{IV}. Finally, the deprotonation of **8iv** generated the desired product **8c**.

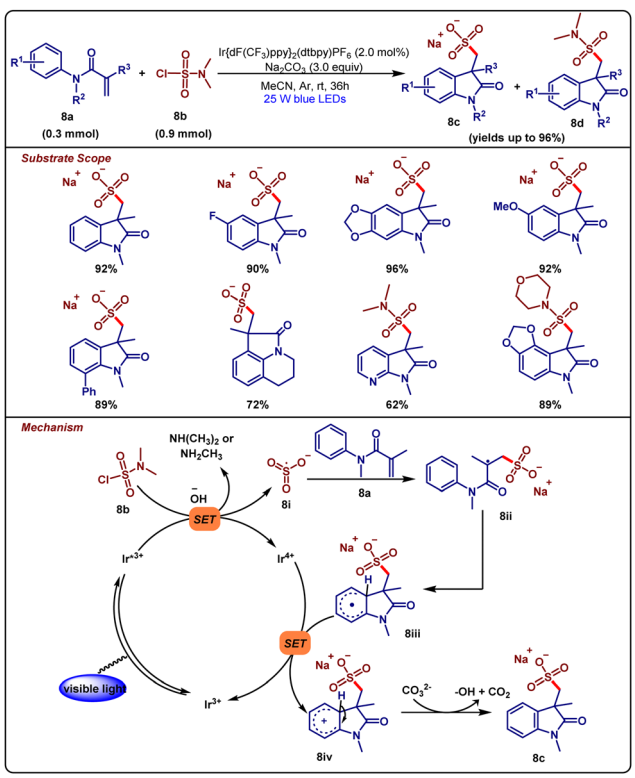

Scheme 8 Photoredox-catalyzed tandem cyclization of electron-deficient alkenes *via* sulfonamidation and sulfonation (Wang method).

In 2022, Liu and Huang *et al.*[19] developed a redox-neutral visible-light-induced radical cascade reaction involving *N*-tosyl acrylamide **9a** and acyl oxime esters **9b** to produce acylated indolin-2-ones **9c** using a tandem process that included acyl radical addition, aryl migration, desulfonylation, and cyclization (Scheme 9). Only 1 mol% of Ir(ppy)$_3$ photocatalyst was enough to achieve up to 86% yield of the desired product within 20 h. Acetonitrile was the most effective solvent among acetone, THF, DCE, DMSO, AcO^{n}Bu and toluene for this transformation. However, this method required a higher temperature (80 °C) with respect to other methods. On studying the substrate scope, the authors found that *N*-alkyl-*N*-(phenylsulfonyl)acrylamides with various alkyl group substitutions, such as *n*-propyl, ethyl, methyl, cyclohexyl, and benzyl, reacted smoothly to produce the target products with yields of 70–80%. Moreover, acrylsulfonylamides with substitutions in the *para* position of the aromatic ring were able to undergo the reaction successfully, resulting in the production of the corresponding products in moderate to excellent yields. In addition, a bunch of oxime esters responded to the reaction under the optimized reaction conditions. For a better understanding of the mechanism, radical trapping experiments were carried out in the presence of 1,1-dipenylethene, BHT, and TEMPO and complete inhibition of the reaction was seen in each case. Moreover, a benzoyl radical trapping product was isolated, which confirmed the radical mechanism. The mechanism of the reaction as proposed by the authors, is shown in Scheme 9. Initially, when exposed to visible light, the photocatalyst [Ir^{III}] transformed into its excited state *[Ir^{III}]. This excited state then underwent a single electron transfer (SET) with acyl oxime ester **9b**, resulting in the formation of iminyl radical **9vii** and oxidized [Ir^{IV}] species. Highly reactive iminyl radical **9vii** then dissociated to form acyl radical

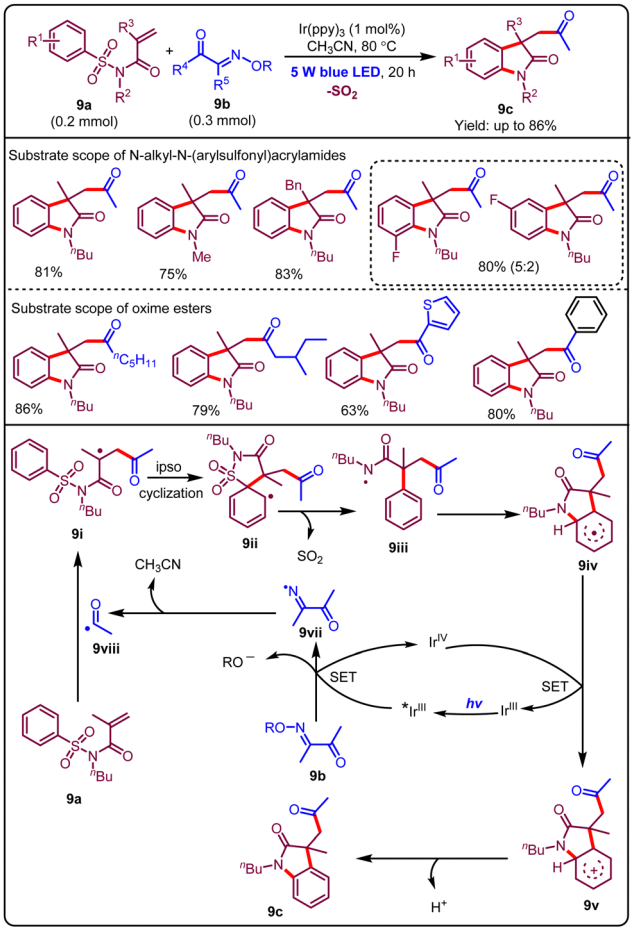

Scheme 9 Light-mediated redox-neutral acylation and arylation of alkenes (Huang method).

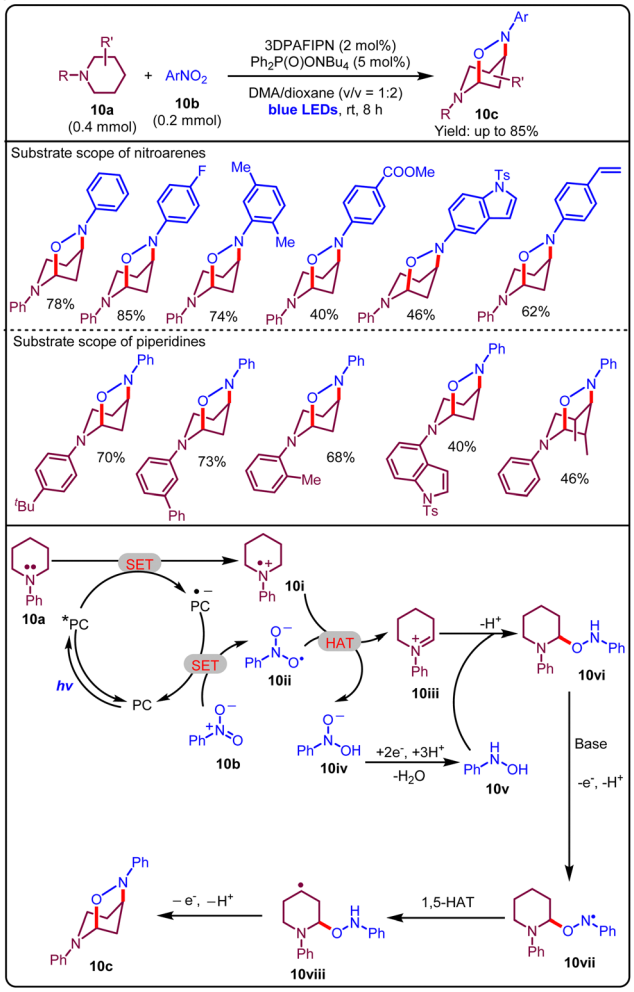

Scheme 10 α,γ-C(sp^3)–H difunctionalization protocol for piperidines in a redox-neutral and visible-light-induced fashion (Zhou and Zhou method).

9viii, which underwent addition reaction with **9a** forming C-center radical intermediate **9i**. Subsequent *ipso*-cyclization and desulfonylation led to the *N*-center intermediate **9iii**. Next, *ortho* cyclization of **9iii** afforded another intermediate **9iv**, which underwent SET oxidization with Ir^{IV} leading to the formation of cationic intermediate **9v**. Finally, the desired product **9c** was obtained by the deprotonation of **9v**.

The Zhou and Zhou group[20] developed a novel and atom-economical α,γ-C(sp^3)–H difunctionalization protocol for piperidines in a redox neutral and visible-light-induced fashion. The authors described that nitroarene **10b** when treated with *N*-arylpiperidine **10a** in the presence of 2 mol% of 3DPAFIPN as catalyst, 5 mol% of $Ph_2P(O)ONBu_4$ as additive, and DMA/dioxane (v/v = 1 : 2) as solvent under blue light irradiation for 8 h, generated a library of α,γ-difunctionalized products **10c** with good yields (with up to 85%) (Scheme 10). The other metal-based photocatalysts, such as $[Ir(ppy)_2(dtbbpy)]PF_6$ and organo-photocatalysts, such as 4CzIPN and DPA2FBN were not as effective as 3DPAFIPN. After successful establishment of the optimized reaction conditions, the authors tried to explore the substrate scope for the reaction. They found that the desired products could be obtained by utilizing *N*-aryl piperidines that had a substituent at the *ortho*-, *meta*-, or *para*-position of the benzene ring. The yields obtained from *N*-aryl piperidines that had an electron-donating substituent were higher compared to those with an electron-withdrawing substituent. In addition to that, *N*-alkylpiperidines were also suitable substrates for this reaction generating the corresponding products under the same optimized reaction conditions. Moreover, this redox-neutral method tolerated a wide range of nitroarenes having various electron-withdrawing and electron-releasing groups leading to the corresponding products with moderate to excellent yields. Furthermore, the authors synthesized an antiproliferative EGFR and $BRAF^{V600E}$ dual inhibitor utilizing this method, which demonstrated the synthetic utility of this method. The control experiments, like Stern–Volmer luminescence quenching experiments, confirmed that *N*-phenylpiperidine initiated the photoredox catalytic cycle as the rate of reductive quenching of *3DPAFIPN by *N*-phenylpiperidine was faster than the rate of oxidative quenching by nitrobenzene. In the radical trapping experiment with TEMPO, suppression of the reaction was observed and the γ-TEMPO adduct was isolated by LCMS, which confirmed a radical mechanism. The proposed mechanism based on the control experiments is depicted in

Scheme 10. Initially, the excited photocatalyst (*PC) was reductively quenched by piperidine substrate **10a** forming nitrogen radical cation **10i** and $PC^{\bullet -}$. Next, $PC^{\bullet -}$ reduced nitrobenzene **10b** to form nitrobenzene radical anion **10ii**, while also regenerating PC. After that, upon the abstraction of an α-hydrogen from **10i** by radical anion **10ii** through a HAT process, iminium intermediate **10iii** and anion species **10iv** were formed. Thereafter, *N*-phenyl hydroxylamine **10v** was generated by a series of reductions and protonations, which underwent an addition reaction with **10iii** to afford **10vi**. Subsequently, the *PC facilitated a base-assisted single-electron transfer process to oxidize intermediate **10vi**, leading to the generation of nitrogen radical species **10vii**. Finally, concomitant 1,5-HAT and SET transfer led to the desired final product **10c**.

In (February) 2023, the Wu group[21] developed a mild, redox-neutral, light-induced methodology for N-radical generation direct from N–H bond activation utilizing quantum dots (QDs) as a catalyst and photosensitizer for the first time. The synthesis explained that aryl halide (or pseudohalide) **11a** interacted with aryl and aliphatic amines **11b** in the presence of CdSe QDs as a photocatalyst and Na_2CO_3 as a base in acetone solvent under blue-light irradiation. The desired aryl or alkyl amine products **11c** were achieved in up to 93% yield within 12–24 h at room temperature (Scheme 11). Optimization studies confirmed that without CdSe, QDs and light, no product was achieved at all. On studying the substrate scope, the authors observed that a broad range of heteroaryl-nitriles, -bromides and -chlorides smoothly responded to the reaction under the optimized reaction conditions. Similarly, a series of secondary arylamines regardless of the nature of the substituents afforded the desired products under the same reaction conditions. Even primary arylamines and alkyl amines were also suitable substrates for this methodology. Gram scale synthesis was also applicable with 85% efficiency.

Very recently in (March) 2023, Oestreich *et al.*[22] developed a room temperature, redox-neutral vicinal dihalogenation of aromatic or alkyl alkenes and alkynes **12b** or **12b'** under photo-mediated conditions. In this synthetic methodology, oxime-based dihalogen surrogate **12a** was used as a halogenating reagent in acetonitrile solvent. Only 1 mol% of photocatalyst $[Ir(dF(Me)ppy)_2(dtbbpy)]PF_6$ was enough to achieve up to 89% yield of the desired vicinal dihalogenated products **12c** (or **12c'**) within 24–36 h (Scheme 12). The authors observed that a library of substituted aliphatic and aromatic alkenes responded to the reaction and afforded good to excellent yields under the optimized reaction conditions. Moreover, the reaction tolerated a wide range of substituted alkynes. In addition to that, both dichlorination and dibromination were easily achievable based on the type of dihalogenating reagents. Furthermore, aryl-substituted allenes were also appropriate substrates of this methodology for giving the mono-1,2-dibrominated products as a single diastereomer. After successfully establishing the substrate scope, they focused on the development of the mechanism based on some control experiments. Without light and photocatalyst, the reaction did not generate the desired product confirming their importance. The radical scavenger TEMPO completely inhibited the reaction and TEMPO-trapping intermediates were isolated using HRMS spectroscopy, which suggested a radical mechanism. Fluorescence-quenching experiments showed that quenching of the fluorescence intensity of the excited iridium photocatalyst was observed only with the addition of a halogenating reagent but not with the alkene, which suggested that the halogenating reagent was reduced at the very beginning step. The mechanism, as depicted in

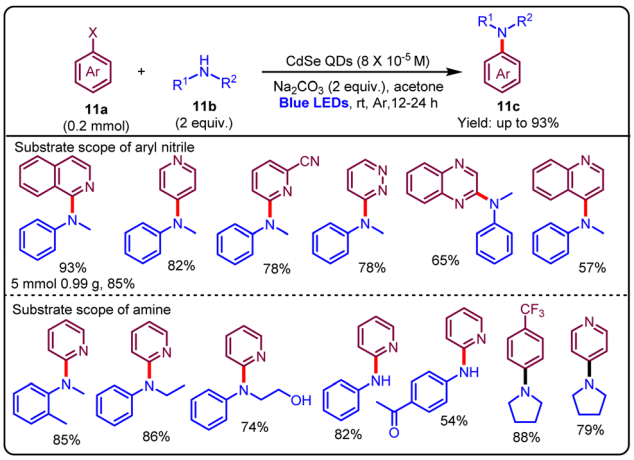

Scheme 11 Redox-neutral visible-light-induced amination of aryl or aliphatic halides and psudohalides (Wu method).

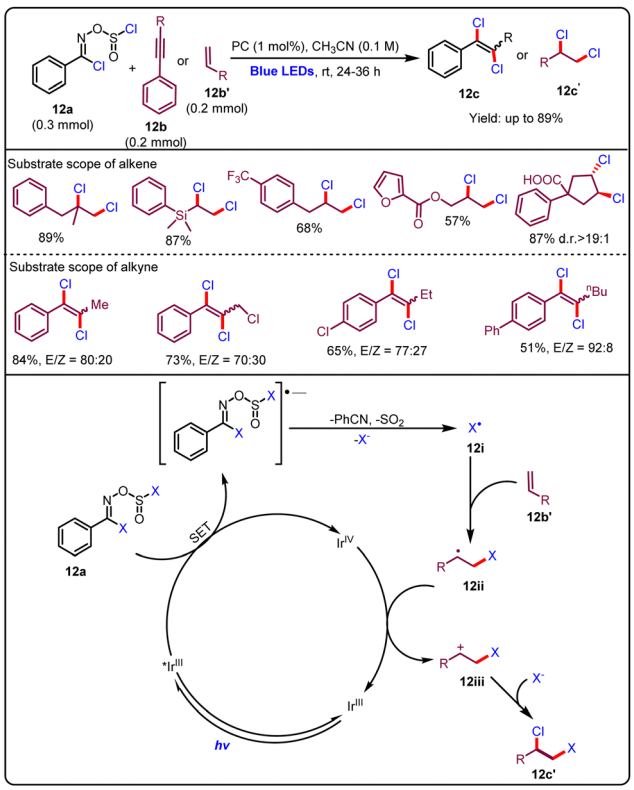

Scheme 12 Visible-light-induced redox-neutral dihalogenation of alkenes and alkynes (Oestreich method).

Scheme 12, was initiated by the excitation of the Ir-catalyst in the presence of blue light. Next, a single electron transfer from $^*Ir^{III}$ to **12a** generated a radical anion, which dissociated to form halogen radical **12i**. Then, the generated electrophilic halogen radical **12i** underwent addition reaction with the unsaturated bond of **12b** leading to the formation of radical intermediate **12ii**. After that, carbocationic intermediate **12iii** was formed by the single electron transfer from **12ii** to Ir^{IV}, along with the preparation of Ir^{III}, completing the catalytic cycle. Finally, the capture of a halide ion by intermediate **12iii** gave the desired product **12c′**.

3. Carbon-centered radical reactions

A few redox-neutral carbon–heteroatom bond formation reactions proceeded *via* formation of carbon-centered radicals in the initial stage of the photoredox cycle.

In 2015, MacMillan's group[23] developed the visible-light-mediated decarboxylative fluorination of aliphatic carboxylic acids under a redox-neutral protocol. The reaction of aliphatic carboxylic acid **13a** with Selectfluor® **13b** in the presence of the catalytic system composed of $Ir[dF(CF_3)ppy]_2(dtbbpy)PF_6$ and Na_2HPO_4 in MeCN/H_2O gave alkyl fluorides **13c** in 99% yield within 6 h (Scheme 13). A wide range of alkyl carboxylic acids, including primary, secondary, and tertiary carboxylic acids were explored under the optimal reaction conditions. Intriguingly, the carboxylic acid substrates bearing heteroatoms underwent faster fluorination within 1–3 hours of reaction time. In order to establish the reaction mechanism, the authors performed a series of Stern–Volmer fluorescence quenching experiments, which proposed that the reduction of Selectfluor® was the initiation point of the photoredox catalytic cycle. Mechanistically, the Ir(III) photocatalyst produced the photo-excited Ir(III)* complex under visible-light irradiation, which then initiated the reduction of Selectfluor® **13b** *via* a single-electron transfer (SET) process and generated Ir(IV)-species **13iv**. On the other hand, this Ir(IV)-species assisted the SET oxidation of base-promoted formation of alkyl carboxylate, and then the extrusion of CO_2 afforded SOMO species **13v** and regenerated photocatalyst **13i**. Finally, the direct fluoride-transfer from Selectfluor® to alkyl radical **13v** led to the desired fluoroalkane **13c** and generated the Selectfluor® radical cation **13iii**.

In 2016, Glorius and co-workers[24] documented visible-light-mediated decarboxylative di- and tri-fluoromethylthiolation of alkyl carboxylic acids **14a** under redox-neutral conditions using phthalimide electrophilic reagent **14b**. The catalytic system consisted of $[Ir(dF(CF_3)ppy)_2(dtbbpy)]PF_6$ as a photocatalyst, CsOBz as a base and C_6H_5F as a solvent for the trifluoromethylthiolation of alkyl carboxylic acids under the irradiation of blue LEDs (λ_{max} = 455 nm). The desired di- and trifluoromethylthiolated products were achieved with up to 94% yield within 4 h (Scheme 14). The reaction was found to be well

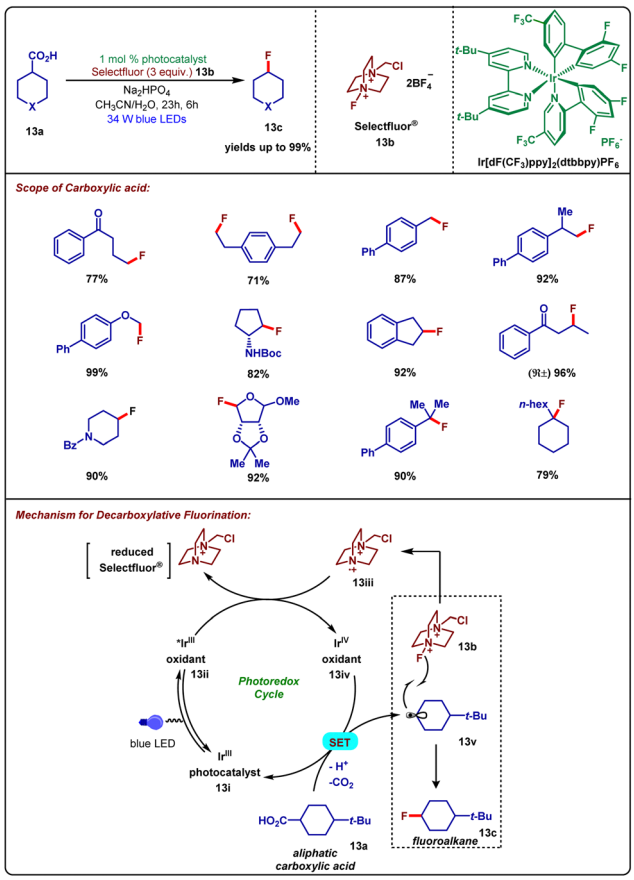

Scheme 13 Photoredox catalyzed decarboxylative fluorination of aliphatic carboxylic acids (MacMillan method).

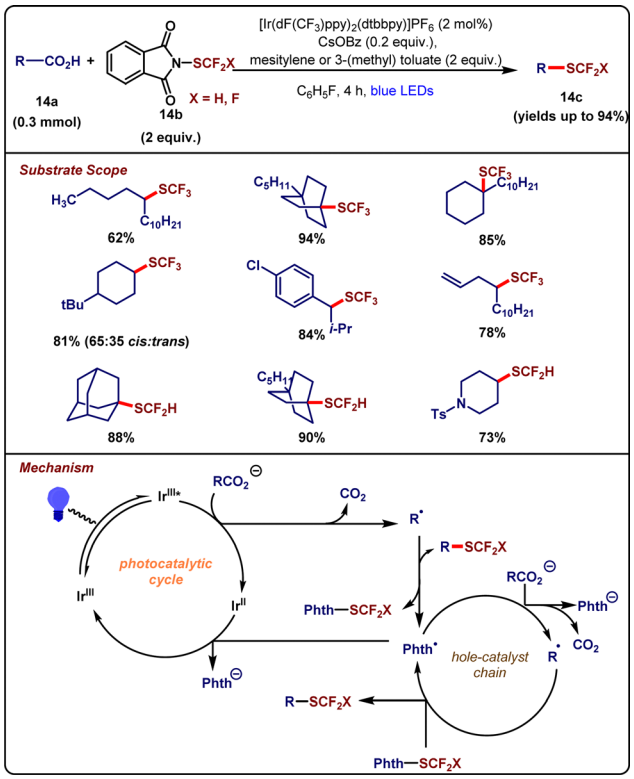

Scheme 14 Photoredox catalyzed decarboxylative di- and tri-fluoromethylthiolation of alkyl carboxylic acids (Glorius method).

tolerated when employing *tertiary*, *secondary*, and benzylic carboxylic acids. Moreover, aryl, protected amines, terminal alkenes, and ketones smoothly participated in the C(sp^3_{alkyl})–SCF_2H bond formation reaction. Furthermore, the scope of this reaction was elaborated to the late-stage functionalization of advanced synthetic intermediates. A plausible catalytic cycle was proposed based on the previous literature reports and Stern–Volmer luminescence quenching experiments and is presented in Scheme 14. The reaction started with the formation of a phthalimidyl radical from **14b** *via* the hole-catalyst chain process, which then participated in single-electron transfer (SET) oxidation with the Ir(II)-complex affording the phthalimide anion and regenerating the photocatalyst. In a parallel reaction, decarboxylation of alkyl carboxylate provided the alkyl radical using the excited state Ir-complex. Subsequently, the transfer of a SCF_3 group reformed the phthalimidyl radical and led to the desired product **14c**.

In 2018, Nevado and co-workers[25] described the remote 1,6-difunctionalization of unactivated alkenes under redox-neutral conditions using a photo-induced cascade strategy. They reported that the carbon-based nucleophiles were used for the functionalization of remote Csp^3–H bonds *via* hydrogen atom transfer (HAT) processes, but oxygen-based nucleophiles were also used for this protocol. According to this protocol, 0.2 mmol of substrate **15a** reacted with 2 equiv. of alkyl bromide **15b** under the irradiation of the photocatalyst $Ir(ppy)_3$ with blue LEDs (34 W) along with AgOAc as a nucleophile and DCM as a solvent at room temperature and produced 1,6-acetoxy alkylation product **15c** in a good yield (Scheme 15). The alkyl halides showcased high functional group tolerance of this redox-neutral remote functionalization because esters, amides, lactones, ketones, and C–Cl bonds were compatible under the optimized route. The olefinic partner with aryl substituents as well as substituents on the aliphatic chain were well tolerated, but fully linear or heteroatom-bridged alkyl chains did not afford the desired product, which suggested the superiority of the Thorpe–Ingold effects in the reaction. The authors performed various supporting experiments such as deuterium levelling experiments and computational studies (DFT) to shed light on the reaction mechanism. The proposed pathway was initiated by photoactivation of the Ir(III)-photocatalyst followed by reduction of the C–Br bond to provide alkyl radical **15i**. Radical **15i** subsequently added to the alkene double bond to deliver C-centred radical **15ii**. After 1,5-hydrogen atom transfer of intermediate **15ii**, more stable benzylic radical **15iii** was formed, which then underwent oxidation in the presence of the Ir(IV)-complex intermediate to produce cationic species **15iv**. At the end, intermediate **15iv** was quenched with either O- or a C-centred nucleophile leading to the formation of desired remote dicarbon- or oxocarbofunctionalization products **15c** (Scheme 15).

In the same year (2018), Stephenson and co-workers[26] accomplished a redox-neutral methodology of alkene (**16a**) aminoarylation with arylsulfonamides (**16b**) as a bifunctional reagent in a diastereoselective fashion (Scheme 16). In this reaction, the authors showcased that arylsulfonylacetamides were competent for both the C–C and C–N bond formation in

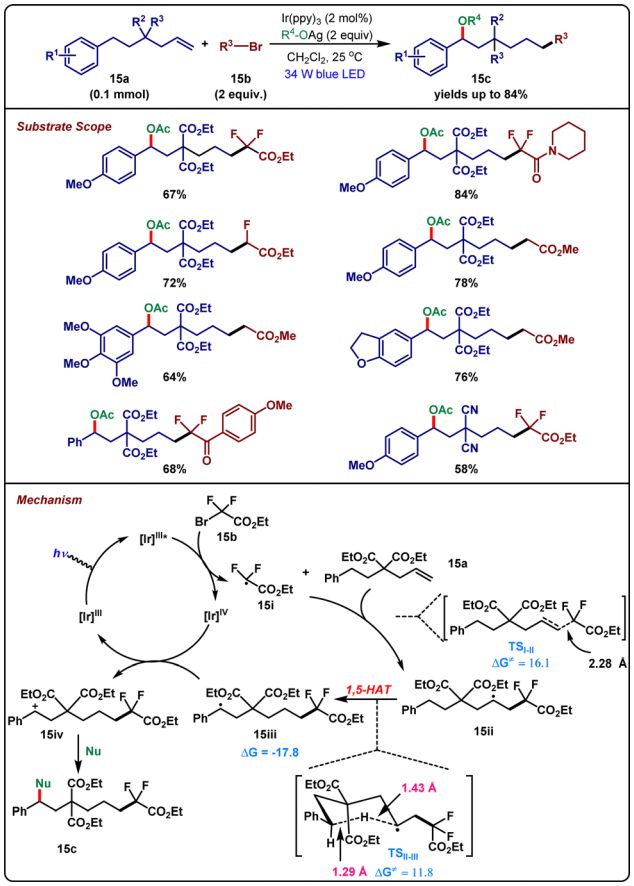

Scheme 15 Photoredox-catalyzed 1,6-difunctionalization of unactivated alkenes (Nevado method).

aminoarylation through the photocatalyzed radical Smiles–Truce reaction. After screening various activating groups, including acyl, amides, and carbamates, acyl groups were found to be suitable for controlling the nucleophilicity of arylsulfonylacetamide. Interestingly, the rate of aminoarylation was increased using 1,2-disubstituted *p*-methoxyphenyl alkenes **16a**. Here, a wide range of substitutions, including 1-naphthyl, 2-naphthyl, 3-thiophenyl, 2-furyl and β-styrene were well tolerated to afford the desired product **16c** in greater than 20 : 1 diastereoselectivity. The key mechanistic studies highlighted that the reaction proceeded *via* single-electron oxidation of alkene **16a** with a photoexcited catalyst ($*Ir^{III}$) forming radical cation **16i**, which subsequently underwent nucleophilic addition to the arylsulfonylacetamide **16b** and afforded the desired β-amino alkyl radical intermediate **16ii**. Then, this radical was poised for regioselective cyclization onto the *ipso*-position of the tethered arene ring to generate intermediate **16iii**. Finally, homolytic fragmentation of the C_{Ar}–S bond followed by the extrusion of SO_2 afforded the aminoarylated product **16c**.

In 2019, Gao and co-workers[27] reported a photo-induced methodology for the borylation of aryl sulfonium salt **17a** using bis(pinacolato)diboron **17b** as a borylating agent *via* C–S bond activation. In this transformation, the combination of light and pyridine was found to be appropriate to produce the optimum

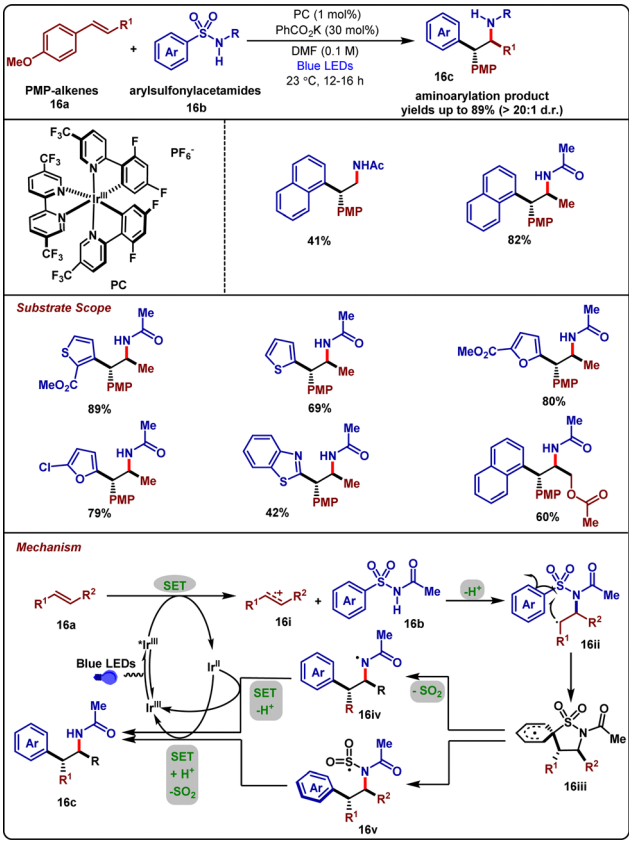

Scheme 16 Photoredox-catalyzed diastereoselective alkene aminoarylation with arylsulfonamides (Stephenson method).

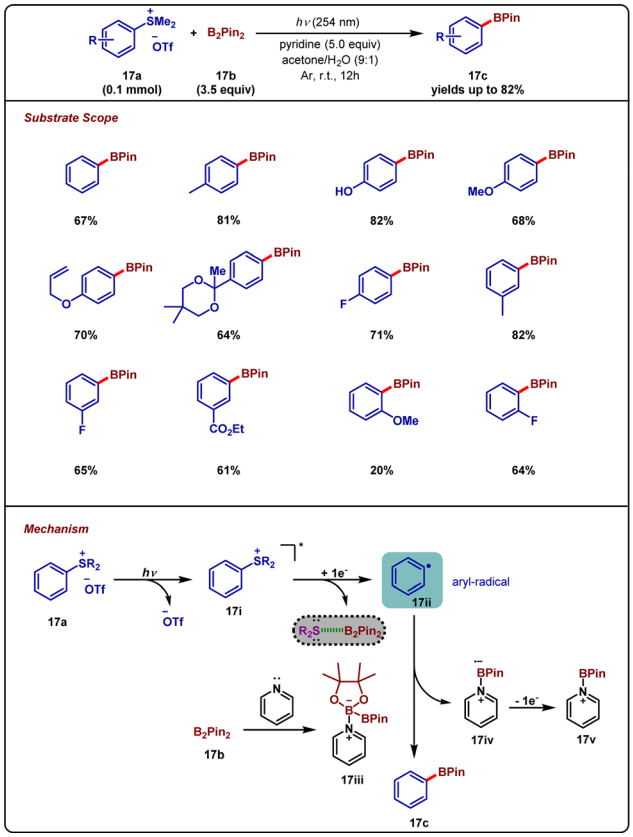

Scheme 17 Photoredox-catalyzed borylation of aryl sulfonium salt (Gao method).

result. The desired borylated products **17c** were achieved in up to 82% yields within 12 h at room temperature (Scheme 17). Under the optimized reaction conditions, a library of aryl sulfonium salt-bearing electron-donating groups and electron-withdrawing groups were tested and most of these substrates showed good activity toward the borylation reaction. Moreover, the authors performed various supporting experiments to gain significant insights into the mechanism for the synthesis of arylboronate esters. These experiments, including the use of radical scavenger and *S*-motif capturing experiments, strongly suggested a radical-based C–S scission mechanism to be operative. The radical process was initiated by the photoexcitation of aryl sulfonium salt **17a** and generated excited state **17i**. Subsequently, C(sp^2)–S bond cleavage produced aryl-radical **17ii** *via* a single-electron transfer (SET) process in the presence of B_2Pin_2 and released the dialkryl-thioether. In the meantime, the boron center of B_2Pin_2 **17b** coordinated with pyridine to form the activated borylating complex **17iii**. Then, the boron group transferred to the aryl radical **17ii** furnishing the desired borylated product **17c** followed by the removal of pyridine-complexed boryl-radical **17iv**. Finally, intermediate **17iv** underwent SET oxidation leading to the formation of pyridinium ion **17v**.

In 2020, an unusual α-nucleophilic addition of α,β-unsaturated carbonyl compounds to form C–O bonds was described by Kang and co-workers.[28] With the use of diphenyldibenzocarbazole (**CBZ6**) as the photocatalyst and water or MeOH as a nucleophile, the regioselective α-nucleophilic oxygenation products of acrylamides were isolated in excellent yields (Scheme 18). After using several PCs such as $Ru(bpy)_3Cl_3$, *fac*-$Ir(ppy)_3$, Eosin Y, Rhodamine B and Rhodamine 6G, **CBZ6** was found to be the most suitable organo-photocatalyst for this reaction protocol. The reduction potential of the excited state of **CBZ6** was found to be −1.92V (*vs.* SCE), higher than that of the metal-based photoredox catalysis, which facilitated umpolung α-nucleophilic addition to α,β-unsaturated amides rather than β-addition products. The authors presented ample scope of various amides to afford the corresponding α-methoxyl amides in very good yields. Besides this, a wide range of alcoholic nucleophiles were well tolerated under the optimized reaction conditions. Importantly, phenols and acetic acid were less reactive under acidic conditions, hence providing the products in less yields. The authors showed that α-fluorination of amides was also feasible in this protocol. To shed light on the reaction mechanism of this methodology, several mechanistic experiments were performed, which led to the following mechanistic proposal. Initially, acrylamide **18a** captured one electron from excited **CBZ6*** to form radical anion **18i** and **18i′** followed by protonation affording radical **18ii** and generated the radical cation of **CBZ6**. Then, the ET oxidation of **18ii** with the radical cation of **CBZ6** produced the cationic intermediate **18iii**, which

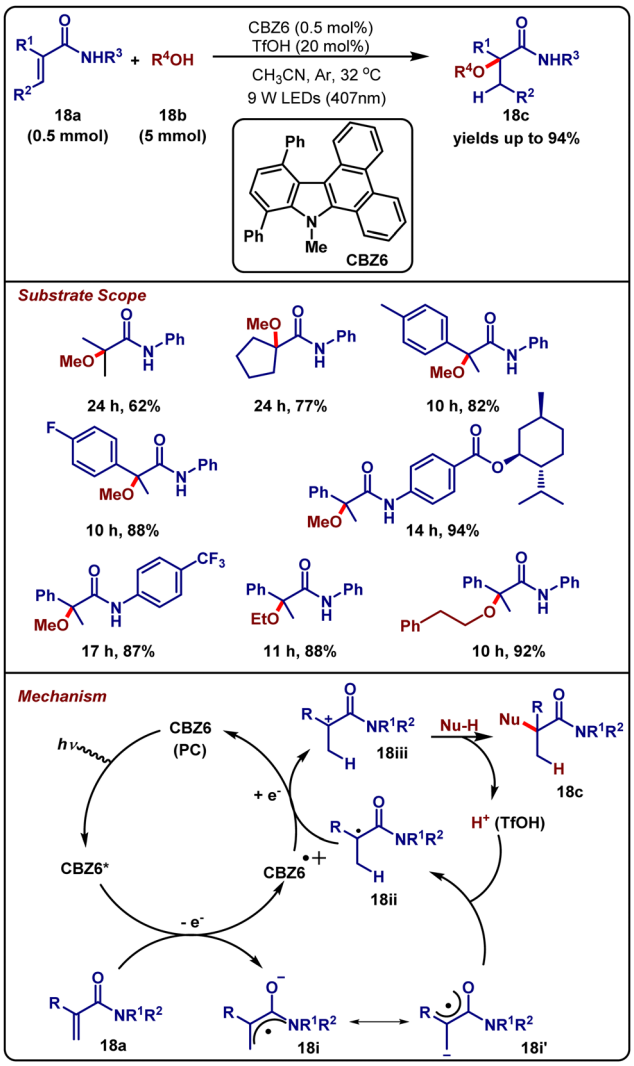

Scheme 18 Photoredox-catalyzed α-nucleophilic addition of alcohols to α,β-unsaturated carbonyl compounds (Kang method).

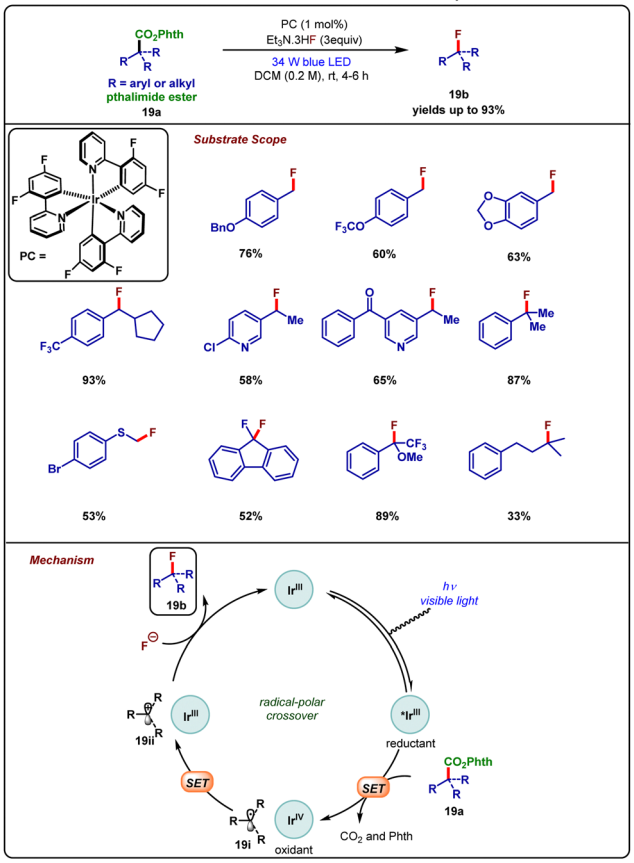

Scheme 19 Photoredoxcatalyzed decarboxylative nucleophilic fluorination of *N*-hydroxyphthalimide esters (Doyle method).

was then quenched by the nucleophiles to form the desired product **18c** and completed the catalytic cycle by the regeneration of the **CBZ6** photocatalyst (Scheme 18).

In 2020, Doyle's group[29] reported a redox-neutral strategy for the decarboxylative nucleophilic fluorination of *N*-hydroxyphthalimide esters **19a** *via* radical-polar cross-over enabled by photo-redox catalysis (Scheme 19). Here, [Ir(dF-ppy)$_3$] as the photocatalyst and Et$_3$N·HF as the electrophilic fluorine source gave the optimum results. This protocol explored various phthalimide esters bearing electron-donating groups under these reaction conditions. Intriguingly, electron-withdrawing substrates afforded fluorinated products in lower yields because the oxidation of the radical to the cation was reluctant due to electron-withdrawing substituents. The limitation of this nucleophilic fluorination was that the secondary benzylic fluorides gave styrene as a by-product. To shed light on the reaction mechanism of this nucleophilic fluorination, several mechanistic experiments were performed, including radical trapping and cation trapping experiments and the authors also developed a radiochemical protocol, which led to the following mechanistic proposal. Initially, photoexcited Ir(III) underwent single-electron transfer with *N*-hydroxyphthalimide ester **19a** and resulted in the phthalimide ester radical anion. Subsequently, the removal of CO_2 produced carbon-centered radical **19i**. Then, radical intermediate **19i** was oxidized by photocatalyst Ir(IV), forming carbocation **19ii** and regeneration of the Ir(III) photocatalyst took place. At the end, the carbocation was quenched with the fluoride source and furnished the desired alkyl fluoride **19b**.

In 2020, Chen's group[30] reported a visible-light-mediated radical multicomponent reaction for the synthesis of indolines *via* a redox-neutral protocol (Scheme 20). In this process, 2-vinylanilines **20a**, sulfonyl chlorides **20b** and sulfur ylides **20c** were irradiated using blue LEDs (7 W) for the synthesis of sulfonated indolines **20d** with up to 97% yield within 9 h. The reaction system was composed of [Ru(bpy)$_3$Cl$_2$]·6H$_2$O as the photocatalyst, K$_2$CO$_3$ as the base and DCM as the solvent. A library of sulfonated indoline compounds was synthesized using this methodology and this method showed high functional group tolerance. Even heterocyclic moieties present in sulfur ylides also worked well under the optimized reaction conditions. Similarly, substituents like electron-donating and electron-withdrawing groups bearing *N*-substituted 2-vinylanilines were well tolerated. The control experiments revealed that the reaction proceeded through radical addition as the key step rather

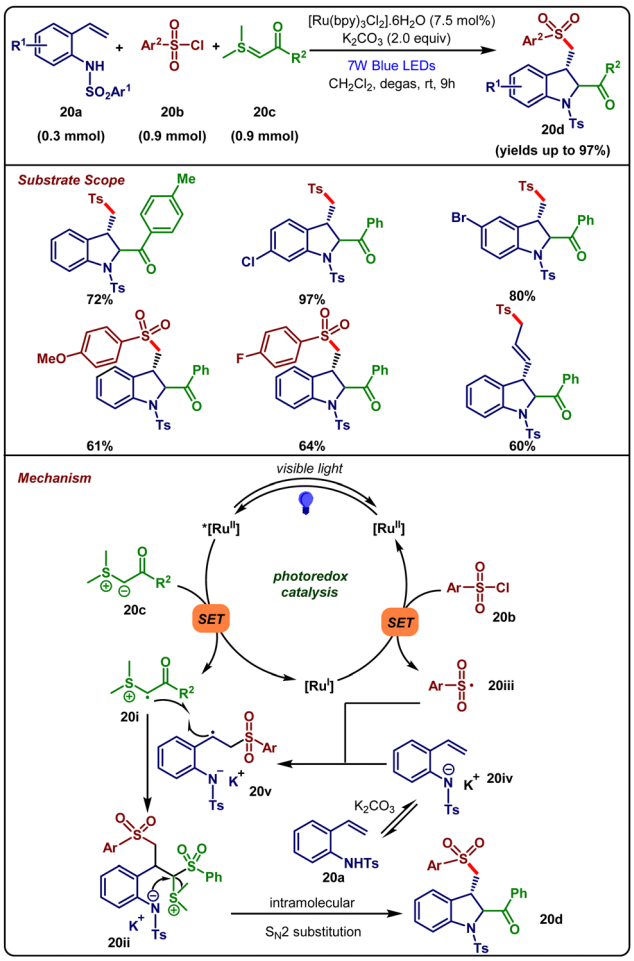

Scheme 20 Photoredox-catalyzed radical multicomponent reaction for the synthesis of indolines (Chen method).

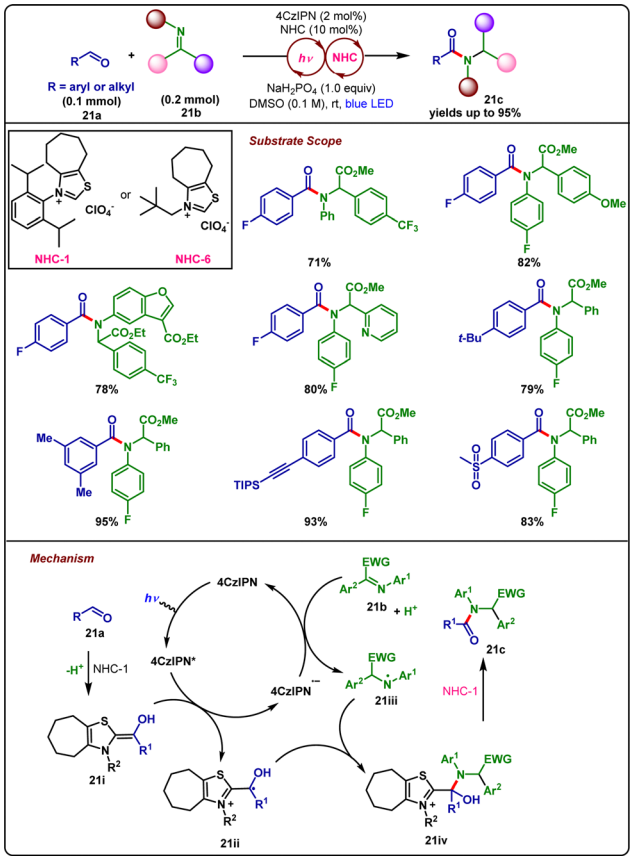

Scheme 21 NHC-mediated photoredox-catalyzed C–N bond formation (Shu method).

than aza-*o*-quinonemethide (aza-*o*-QM). Based on the previous literature reports and experimental studies, the catalytic cycle was initiated with SET oxidation of the sulfur ylide by the excited [*Ru^{II}] leading to the generation of radical **20i**. Then, the reduced photocatalyst [Ru^{I}] underwent SET oxidation by sulfonyl chlorides **20b** to generate the electrophilic sulfonyl radical **20iii**. Subsequently, radical **20iii** *in situ* reacted with 2-vinylaniline salt **20iv** to produce another radical intermediate **20v**. Finally, benzyl radical **20v** and radical **20i** combined through radical–radical coupling leading to the formation of intermediate **20ii**. Subsequent intramolecular SN^2 substitution solely offered the desired cyclized product **20d.**

In 2020, Shu *et al.*[31] disclosed a procedure for C–N bond formation reaction enabled by the dual catalysis of visible light and N-heterocyclic carbene (NHC) at room temperature. A wide range of substituted amides **21c** were thus obtained when aryl imines **21b** reacted with aromatic aldehydes **21a** using 4CzIPN (1,2,3,5-tetrakis(carbazole-9-yl)-4,6-dicyanobenzene) and NHC-6 as catalysts and Na_2HPO_4 as the base in DMSO solvent under the irradiation of a 30 W blue LED (Scheme 21). Moreover, control experiments suggested that both the NHC catalyst and 4CzIPN were essential for the desired C–N coupling product. Both electron-donating and electron-withdrawing substituents were well tolerated on the aryl imine substrate to give the desired amides under the optimized reaction conditions. The aromatic aldehydes bearing different substituents afforded the C–N cross-coupled product in good to excellent yields. Different control experiments were performed to gain insight into the mechanism, including radical quenching, radical monitoring, light on–off and cross-over experiments. Mechanistically, the reaction began with the formation of Breslow intermediate **21i** generated from the condensation reaction between aldehyde **21a** and the N-heterocyclic carbene catalyst (NHC). On the other hand, the excited photocatalyst (4CzIPN*) underwent reductive quenching by intermediate **21i** to give radical cationic intermediate **21ii** and the reduced photocatalyst ($4CzIPN^{\bullet-}$). Next, imine **21b** could undergo reduction by $4\text{-CzIPN}^{\bullet-}$ to generate *N*-centered radical **21iii** and photocatalyst 4-CzIPN could be regenerated at the same time. Intermediates **21ii** and **21iii** participated in the radical–radical cross-coupling C–N bond-forming process to produce **21iv** and subsequently, removal of the NHC catalyst yielded the final amide product **21c.**

The next year, in 2021, the MacMillan group[32] developed a decatungstate-photocatalyzed direct conversion of robust aliphatic $C(sp^3)$–H bonds **22a** into their corresponding alkyl sulfinic acids **22c** under redox-neutral conditions. In this

method, various SO_2 surrogates were tested but inexpensive aqueous sulfur dioxide **22b** was the most suitable. The most suitable conditions for the reaction were 1 mol% of sodium decatungstate ($Na_4[W_{10}O_{32}]$) photocatalyst in acetonitrile/water under PR160 40 W Kessil 390 nm light for 4–8 h. The generated sulfinic acids **22c** could be easily converted to the corresponding benzyl sulfones **22d** with up to 86% yield in one-pot by the reaction with benzyl bromide (Scheme 22). The authors then explored its substrate scope based on the optimized reaction conditions. They found that a variety of cyclic hydrocarbons containing electron-withdrawing groups responded to this method affording moderate to excellent yields of the desired products. Moreover, outstanding selectivity was seen for the more electron-rich, sterically accessible positions. Medicinally relevant bicyclic scaffolds, such as tricyclic imide and brominated norbornane derivatives, were smoothly sulfinylated at the most accessible, electron-rich position as a single regioisomer. In addition to that, heterobicyclic scaffolds also took part in this method under the same reaction conditions. The gram-scale synthesis was also an extra advantage for this method. Based on some control experiments and energy calculations with the help of DFT, the authors proposed the most suitable mechanism for the reaction, as shown in Scheme 22. Initially, the highly reactive excited state $*[W_{10}O_{32}]^{4-}$ might be obtained through the rapid relaxation of the decatungstate anion upon near-UV excitation. Next, as the oxygen-centered hole in $*[W_{10}O_{32}]^{4-}$ was electrophilic, HAT (hydrogen atom transfer) would occur selectively at the β-position of the more electron-rich cyclopentanone **22a**, resulting in the formation of alkyl radical **22i** and reduced decatungstate ($[W_{10}O_{32}]^{5-}$). Next, sulfur dioxide **22b** rapidly picked up the newly formed alkyl radical **22i** and generated sulfonyl radical **22ii**. To close the cycle, $[W_{10}O_{32}]^{5-}$ would undergo disproportionation to yield the doubly reduced decatungstate ($[W_{10}O_{32}]^{6-}$), which would then undergo single-electron reduction by sulfonyl radical **22ii** and form corresponding sulfinate **22c**. Subsequent protonation under sufficiently acidic conditions would result in the generation of sulfinic acid. On the other hand, sulfinate **22c** formed the desired product **22d** on reaction with BnBr in a basic medium.

In 2022, Feng and co-workers[33] demonstrated the photoredox catalyzed C(sp^3)–heteroatom bond formation reaction *via* ring opening functionalization of electronically unbiased aryl cyclopropanes **23a**. After irradiating several photocatalysts in the presence of a blue LED, the acridinium photocatalyst ($E_{1/2}$(Acr*/Acr$^-$) = +2.08 V *vs.* SCE) proved to be the best to offer product **23c** in up to 95% yield (Scheme 23). The addition of diphenyl disulfide as a hydrogen atom transfer (HAT) reagent was needed for this redox-neutral transformation. Using this methodology, a wide range of sterically congested C–O and C–N bonds were synthesized by C–C bond cleavage. Initially, the aryl cyclopropane was examined with different nucleophiles such as ethanol, $TfNH_2$ and pyrazole. Presumably, electron-rich substituents such as methoxy, alkyl, and phenyl on the phenyl ring of aryl cyclopropane provided the ethers, amides, and α-quaternary substituted heterocycles in good to excellent yields. Next, the oxygen-based nucleophile was also investigated. Primary and secondary alcohols were amenable, but tertiary alcohols did not work under the reaction conditions. Aside from the alcohols, carboxylic acids were also suitable as O-type nucleophiles. Moreover, chlorination and fluorination could occur readily by using 2,6-lutidine hydrochloride and triethylamine trihydrofluoride as nucleophiles, respectively. After the substrate scope investigation, the authors spent their time on

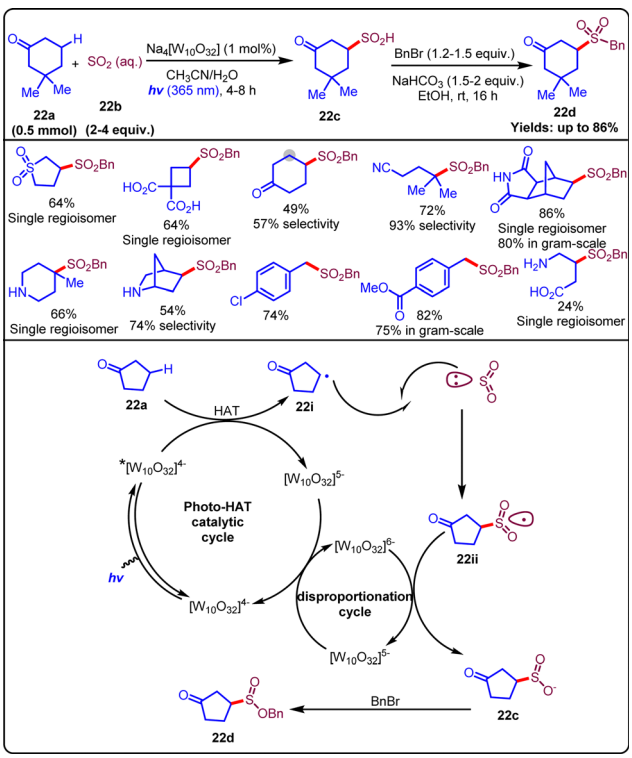

Scheme 22 Redox-neural photocatalyzed C(sp^3)–H sulfinylation (MacMillan method).

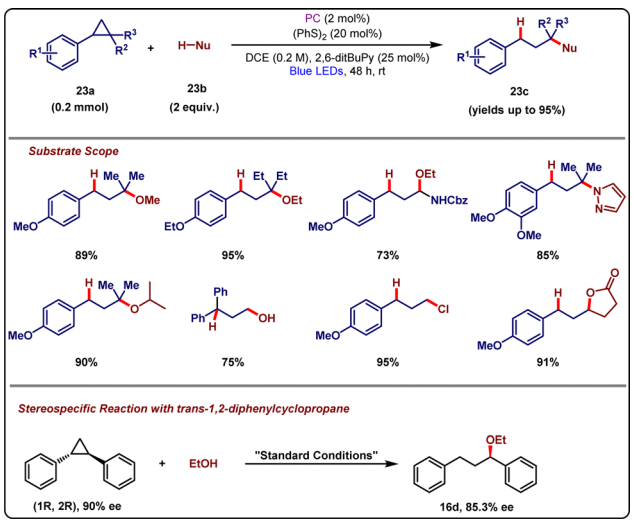

Scheme 23 Photoredox-catalyzed C(sp^3)–heteroatom bond formation (Feng method).

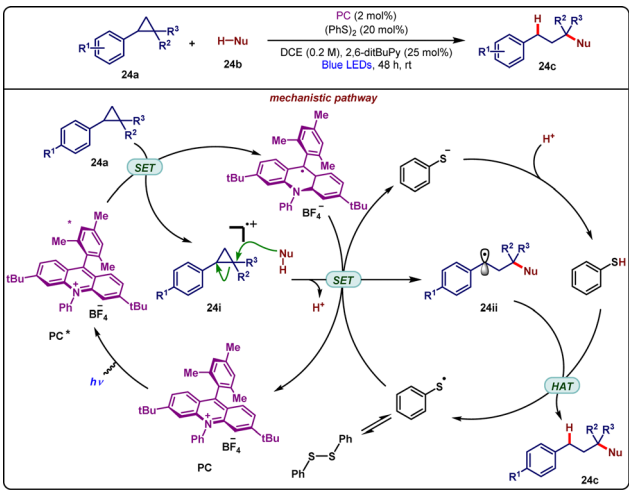

Scheme 24 The plausible mechanism.

finding the intermediates and reaction mechanism. Hence, a series of control experiments were performed to get insight into the mechanism. The TEMPO addition as a radical scavenger did not offer the desired product and also a radical clock experiment provided the ring-opening product, which effectively suggested the formation of a benzylic radical intermediate. Furthermore, the quantum yield (ϕ = 0.182) of the reaction indicated that the radical chain process was not the major pathway. To establish the nucleophilic SN^2 ring opening functionalization, enantioenriched *trans*-1,2-diphenyl cyclopropane **23d** was treated with ethanol under the optimized conditions and formed product **23e** with 85% ee (Scheme 23). Hence, the proposed probable stereochemistry scrambling occurred through either triplet energy transfer or SET-induced reversible ring cleavage of cyclopropane. Finally, with the help of DFT studies and previous experiments, the suggested mechanism began with the generation of an excited state acridinium catalyst, which was then reductively quenched by aryl cyclopropane **24a** and formed aryl cyclopropyl cation radical **24i**. Subsequently, the nucleophilic attack of the nucleophile regioselectively produced the ring-opened carbon-centered radical species **24ii**. Lastly, the hydrogen atom transfer (HAT) from thiol produced the desired product **24c** and active HAT reagent was regenerated *via* reduction of the thiol radical by the acridinium radical photocatalyst followed by proton transfer, closing the catalytic cycle (Scheme 24).

4. Mixed carbon- and heteroatom-centered radical reaction

A few redox-neutral carbon–heteroatom bond formation reactions proceeded *via* simultaneous formation of carbon as well as heteroatom-centered radical ions at the initial stage of the photoredox cycle.

In 2020, Wu's group[34] demonstrated a C–N bond formation reaction *via* direct radical–radical cross-coupling empowered

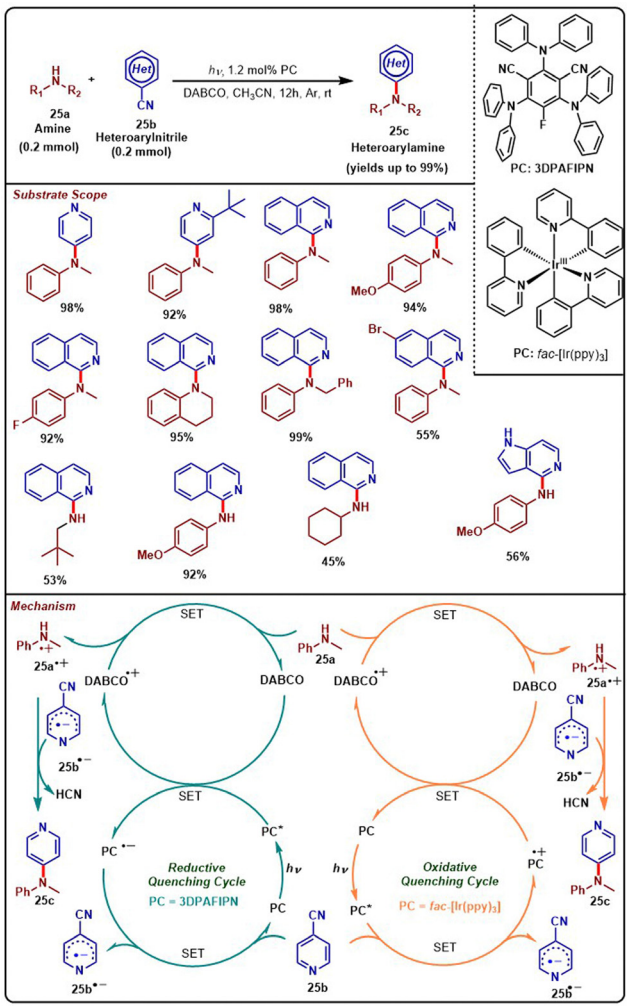

Scheme 25 C–N bond formation *via* radical–radical cross-coupling in the presence of photoredox catalyst 3DPAFIPN (Wu method).

by visible light photocatalysis. This method overcame the use of transition-metals, external oxidants, or reductants for site-selective access to heteroaryl amines. In contrast, the catalytic system consisting of 3DPAFIPN, DABCO and CH_3CN gave the optimal result for the synthesis of heteroaryl amine **25c** from amine **25a** and heteroarylnitrile **25b** (Scheme 25). In the case of heteroarylnitrile, a wide range of heteroaryl substituents like pyridine, pyrazine, and isoquinoline were well compatible under the standard reaction conditions. Similarly, amine-coupling partners such as secondary and primary aryl amines containing electron-donating and electron-withdrawing groups present in aryl rings gave the desired products in satisfactory yields. However, primary alkyl amines showed no reactivity under these reaction conditions. Several spectroscopic studies were performed to shed light on the reaction mechanism of this transition metal-free manifold, which led to the following mechanistic proposal. Initially, DABCO was oxidized in the presence of excited PC* to produce $DABCO^{\bullet+}$, which subsequently oxidized **25a** to generate amine radical cation $\mathbf{25a}^{\bullet+}$. On the other hand, an alternative oxidative

quenching cycle was reported when *fac*-Ir(Ppy$_3$) was used as the photocatalyst. In that oxidative quenching cycle, first heteroaryl radical anion **25b**$^{\bullet-}$ was produced by excited PC* and it further reacted with radical cation **25a**$^{\bullet+}$ leading to radical–radical cross-coupling product **25c** (Scheme 25).

In 2022, Nicewicz's group[35] did a detailed mechanistic investigation on the amination of electron-neutral as well electron-rich arenes using organic photoredox catalysis (Scheme 26). The authors have termed this type of reaction as ''cation radical accelerated nucleophilic aromatic substitution'' (CRA-S$_N$Ar). The authors have reacted a variety of aryl fluorides with pyrazole in the presence of an organo-photoredox catalyst (catalyst A) under the optimized conditions and found that electron-neutral as well electron-rich arenes were well tolerated under the present conditions (Scheme 26). They found that catalyst A was more effective than other catalysts used (catalysts B and C) in this reaction. They began their mechanistic investigations with the reaction between 4-fluorotoluene (**26a**) and pyrazole (**26b**) in the presence of catalyst A (Scheme 26A). Based on the oxidation

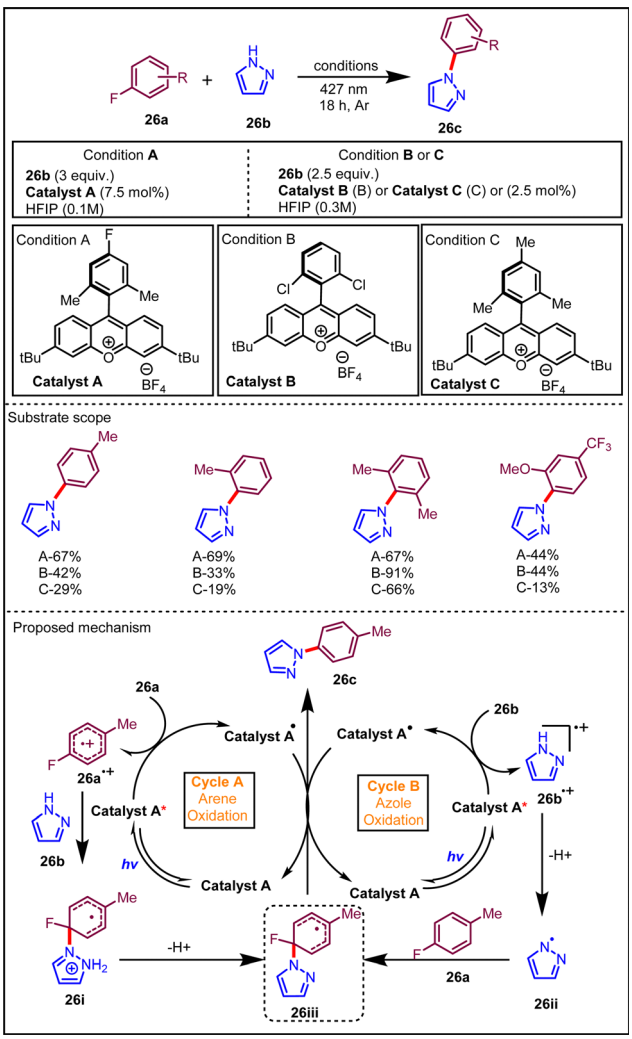

Scheme 26 The amination of electron-neutral as well electron-rich arenes using organic photoredox catalysis (Nicewicz method).

potentials of 4-fluorotoluene (**26a**, $E_{p/2}$ = +2.24 V *vs.* SCE) and pyrazole (**26b**, $E_{p/2}$ = +2.21 V *vs.* SCE) as reported by the authors, there are two possible mechanistic pathways (Scheme 26B). Both catalytic cycles are initiated with the irradiation of catalyst A, giving rise to an excited-state of species (*i.e.*, catalyst A*) $\left(E^{*\mathrm{red}}_{1/2} = +2.57 \text{ V } \textit{vs.}\text{ SCE}\right)$. The oxidation of **26a** by catalyst A*, as shown in Cycle A, led to arene cation radical **26a**$^{\bullet+}$. This electrophilic species could then be reacted with **26b** at the fluorine-bearing carbon to give a cation radical **26i**. Deprotonation and removal of fluoride *via* reduction would give the observed substitution product **26c** and regenerate the photocatalyst in a redox-neutral pathway. Alternatively, the oxidation of **26b** could also be possible to give aminium cation radical (**26b**$^{\bullet+}$) as shown in Cycle B. Next, a nitrogen centered radical (**26ii**) would be generated *via* rapid deprotonation of **26b**$^{\bullet+}$. This nitrogen centered radical **26ii** could then react with fluoroarene **26a** and produce the same key intermediate **26iii**, and the catalytic cycle would close in a manner like Cycle A. It is worth mentioning here that the authors have investigated this reaction with a combination of kinetic, spectroscopic, electrochemical, and computational techniques to confirm the following reaction pathways and moreover, extended it to other amination methods.

5. Carbene intermediate-assisted reaction

In 2022, Jin *et al.*[36] presented a metal-free method for the dual functionalization of C(sp^3)–H bonds in tertiary amines, which involved the use of a diazoester as a hydride-acceptor precursor. The process involved hydride-transfer-induced dehydrogenation followed by cycloaddition and was carried out under mild, redox-neutral and photo-mediated conditions. According to this article, reaction of 1 equiv. of aromatic *N*-hydroximoyl chlorides **27a** with 2.4 equiv. of tertiary amines **27b** in the presence of 2 equiv. of diazoester in DCM solvent at room temperature led to the formation of desired product **27c** with up to 84% yield within just 1 h (Scheme 27). Use of other than blue light, such as white, purple, red and green or UV led to lower yields of the desired products. In addition to that, no product was formed at all in the absence of light. Moreover, substitution on the phenyl ring of the ester resulted in lower yields of the desired products. After successful establishment of the optimized reaction conditions, the authors tried to explore the substrate scope. They found that various substituted aromatic *N*-hydroximoyl chlorides responded to the reaction without significant positional effects and generated moderate to excellent yields. However, in the given reaction, it was observed that the electron-withdrawing groups provided slightly higher yields of the corresponding products compared to the electron-donating groups. Furthermore, aliphatic *N*-hydroximoyl chlorides also showed compatibility under the optimized reaction conditions. On the other hand, the difunctionalized products could also be easily synthesized from tertiary amines with

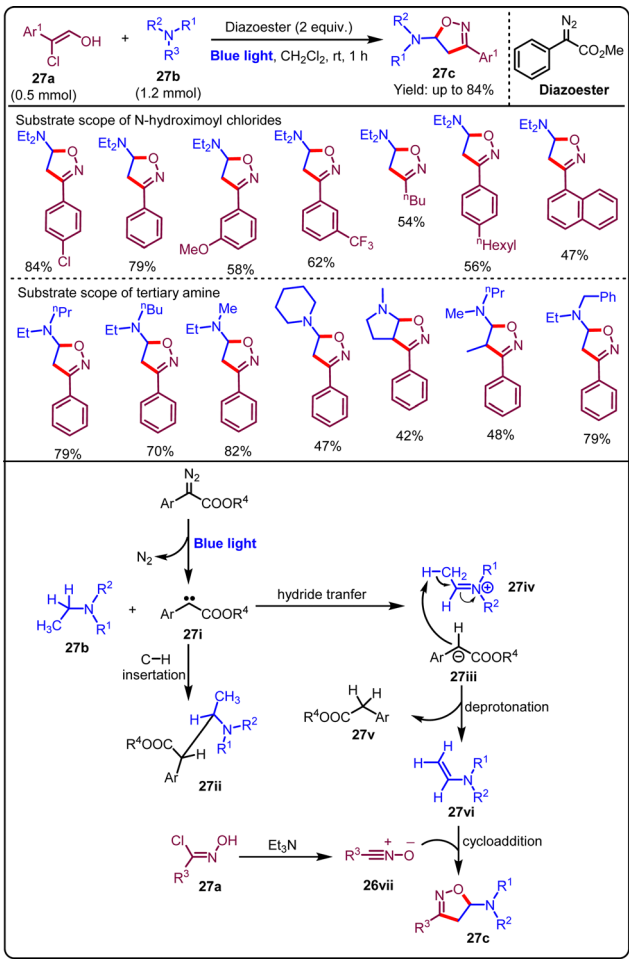

Scheme 27 Redox-neutral visible-light-induced dual C(sp^3)–H bond functionalization of tertiary amines (Jin method).

varying lengths of aliphatic chains through the given chemical transformation. One point to be mentioned here is that the yields of the difunctionalized products were comparatively lower with branched tertiary amines as compared to linear tertiary amines, which could be attributed to the steric hindrance caused by the branching of the aliphatic chains. Control experiments, like radical trapping experiments, KIE, *etc.* were used to develop the mechanism and the most suitable mechanism proposed by the authors is depicted in Scheme 27. At the beginning, when exposed to blue light, the diazoester became activated to a higher energy excited state, which then led to the generation of reactive free carbene species **27i** through the release of N_2. Reactive carbene species **27i** could act as an electrophile and abstract the hydride adjacent to the nitrogen of **27b**, resulting in the formation of ion pairs **27iii** and **27iv**, along with by-product **27ii**. The deprotonation of β-C–H of iminium ion **27iv** led to the release of enamine intermediate **27vi** and protonated compound **27v**. Additionally, the tertiary amine could promote HCl elimination from **27a** to form nitrile oxide **27viii**, which underwent 1,3-dipolar cycloaddition with enamine **27vi** producing the final isoxazoline product **27c**.

6. Combination of photocatalysis with other metal catalysis: metallaphotoredox catalysis

Recently, the merger of photocatalysis and metal catalysis, known as metallaphotocatalysis, has been gaining tremendous importance.[2k,10a,37] In 2015, MacMillan and coworkers[38] reported a redox neutral efficient room-temperature carbon–oxygen bond formation methodology of abundant alcohols **28a** and aryl bromides **28b** using the merger of photoredox and nickel catalysis. The reaction required Ir[dF(CF_3)ppy]$_2$(dtbbpy)PF_6 as a photocatalyst, $NiCl_2$·glyme, dtbbpy, quinuclidine, K_2CO_3 and blue light irradiation. The desired C–O coupling products **28c** were achieved with up to 96% yield within 24 h (Scheme 28). After achieving the optimal conditions, the authors then tried to focus on the substrate scope. They found that a broad range of bromoarenes containing a variety of functional groups responded to the reaction under the optimized reaction conditions. Moreover, bicyclic aryl bromides and heteroaryl bromides were also suitable substrates for this method. On the other hand, exploration of alcohol substrates demonstrated that a series of primary and secondary alcohols afforded the desired ether products with good to excellent yields irrespective of the nature of nucleophilicity. When a substrate contained both a primary and secondary alcohol, the less hindered site was primarily arylated. Control experiments confirmed that a reductive elimination to form a C–O bond arose in the presence of photocatalysts and light. In addition to that, both cyclic voltammetry and Stern–Volmer fluorescence quenching experiments also suggested a single-electron transfer oxidation–reduction process. The proposed mechanism, as depicted by the authors, is shown in Scheme 28. Initially, oxidative addition of the Ni(0)-complex to aryl bromide **28b** led to the formation of Ni(II) aryl complex intermediate **28i**. Next, Ni(II) aryl alkoxide **28ii** would be formed through a ligand exchange reaction. Simultaneously, visible-light exposure of the heteroleptic iridium(III)-photocatalyst might result in the long-lived photoexcited *Ir(III) state, which oxidized Ni(II)-intermediate **28ii** to Ni(III)-intermediate **28iii** and itself was reduced to Ir(II). The desired aryl ether product **28c** was achieved *via* reductive elimination of intermediate **28iii**. Finally, a second SET event between the Ir(II)-complex and Ni(I)-complex managed to complete both of the catalytic cycles.

In the same year, Lu and Xiao *et al.*[39] reported a room temperature redox-neutral C–P bond formation reaction of aryl iodides **29a** with diarylphosphine oxides **29b** in the presence of dual Ni- and Ru-catalysis. The blue-light-induced methodology afforded up to a 91% yield of the desired product **29c** when 2 mol% of $Ni(cod)_2$, 5 mol% of $[Ru(bpy)_3Cl_2]\cdot 6H_2O$ and Cs_2CO_3 were used as the metal catalyst, photoredox catalyst and base, respectively, in methanol solvent for 24 h (Scheme 29). The authors observed that other Ni-catalysts, such as $NiCl_2(PPh_3)_2$ and $NiCl_2$·glyme afforded lower yields of the desired products. Similarly, Ir-photocatalysts were not as efficient as Ru-photocatalyst. Based on the optimized reaction conditions, they then explored the substrate scope for this reaction. It was observed

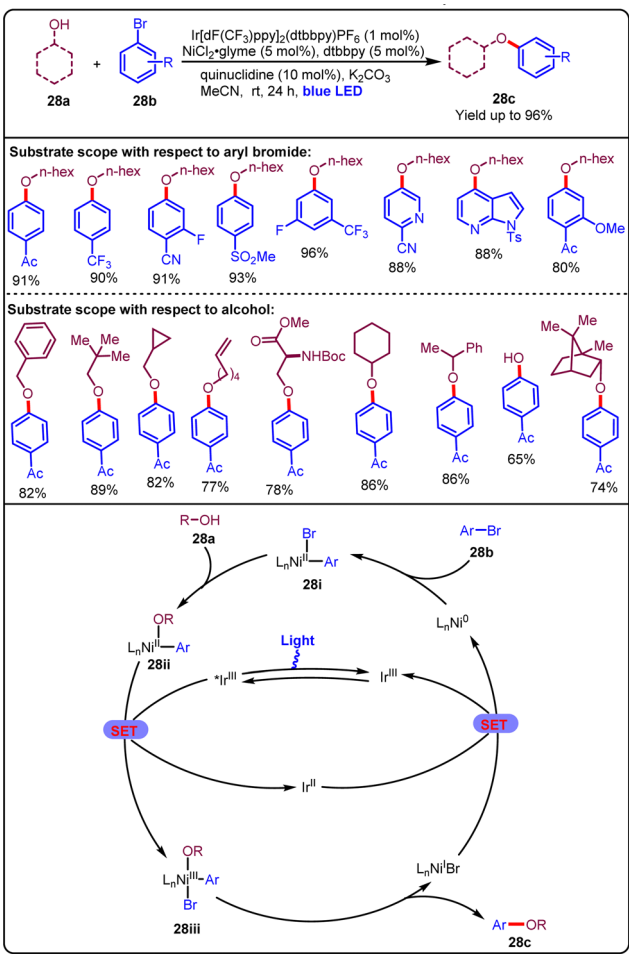

Scheme 28 Visible-light-induced metallaphotoredox catalysis for C–O bond formation (MacMillan method).

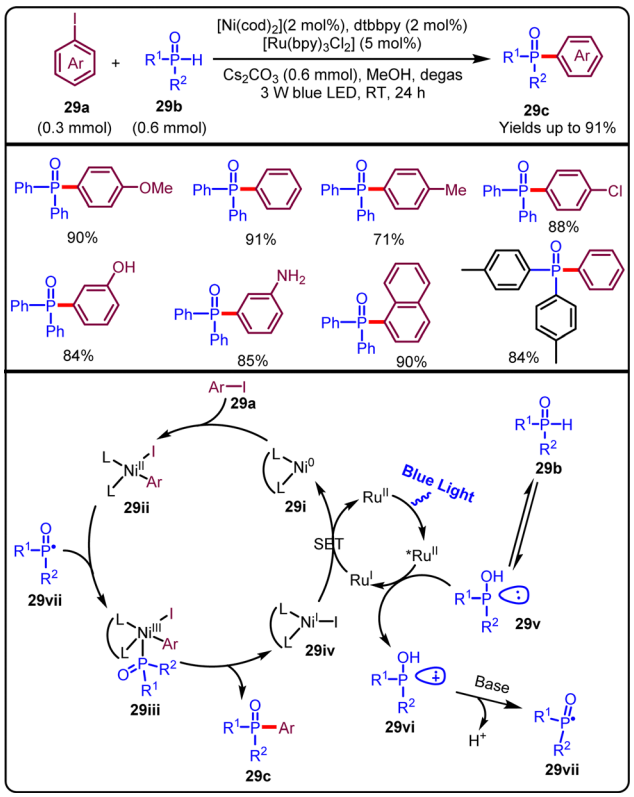

Scheme 29 Visible-light-induced redox-neutral C–P bond formation at room temperature.

that both electron-withdrawing as well as electron-donating groups on iodobenzene efficiently participated in the reaction. Moreover, a broad range of functional groups were well tolerated on the aryl ring of aryl iodide under the same reaction conditions. In addition, methyl-modified secondary phosphine oxide also responded to the reaction affording the desired products. However, dicyclohexylphosphine oxide did not generate the desired products under the best reaction conditions. After successfully demonstrating the substrate scope, the authors tried to focus on the establishment of the mechanism for the reaction. As shown in Scheme 29, initially, the Ru(II) photocatalyst absorbed the blue light irradiation and formed excited *Ru(II). Next, the reductive quenching of *Ru(II) with phosphinous acid **29v** generated radical-cation intermediate **29vi**, which subsequently underwent base-promoted deprotonation leading to P-centered radical intermediate **29vii**. In the meantime, the Ni(0)-catalyst underwent oxidative addition with aryl iodide **29a** to form intermediate **29ii**. After that, the previously generated P-centered radical **29vii** quickly added to **29ii** forming organometallic Ni(III)-complex **29iii**. Thereafter, the desired final product **29c** along with Ni(I) species **29v** was obtained by reductive elimination of **29iii**. Finally, a single-electron reduction of Ni(I) species **29iv** by Ru(I) completed the catalytic cycle. However, according to the authors, another mechanism could be possible involving the addition of P-centered radical intermediate **29vii** to Ni(0) species **29i**.

In 2016, Buchwald and MacMillan *et al.*[40] developed a facile aryl amination methodology by merging of photoredox catalysis with nickel catalysis in the absence of any external oxidizing or reducing agent. According to this method, 1 equiv. of aryl bromides **30a** interacted at room temperature with 1.5 equiv. of alkyl or aryl amine **30b** in the presence of 5 mol% $NiBr_2$·glyme and $Ir[dF(CF_3)ppy]_2(dtbbpy)PF_6$ as the metal catalyst and photoredox catalyst, respectively, in DMA solvent under blue light irradiation. However, DABCO was required for this reaction and worked as a base. The desired arylated amine product **30c** was achieved with up to 96% yield within 24 h (Scheme 30). After successfully achieving the optimal conditions, the authors tried to focus on the scope of the method with various substrates. They found that an extensive range of functional groups were allowed on the amine coupling partner, including alcohols, alkenes, trifluoromethyl groups, sulfonamides and even protected nitrogen atoms. Moreover, nucleophilic amines, such as morpholine, and pyrrolidine responded to the reaction with good efficiencies under the optimized reaction conditions. However, *tert*-butylamine did not afford the desired products due to steric hindrance. Similarly, amines that do not have α-hydrogens were unsuccessful. On the other hand, aryl bromides containing electron-withdrawing, -releasing and -neutral

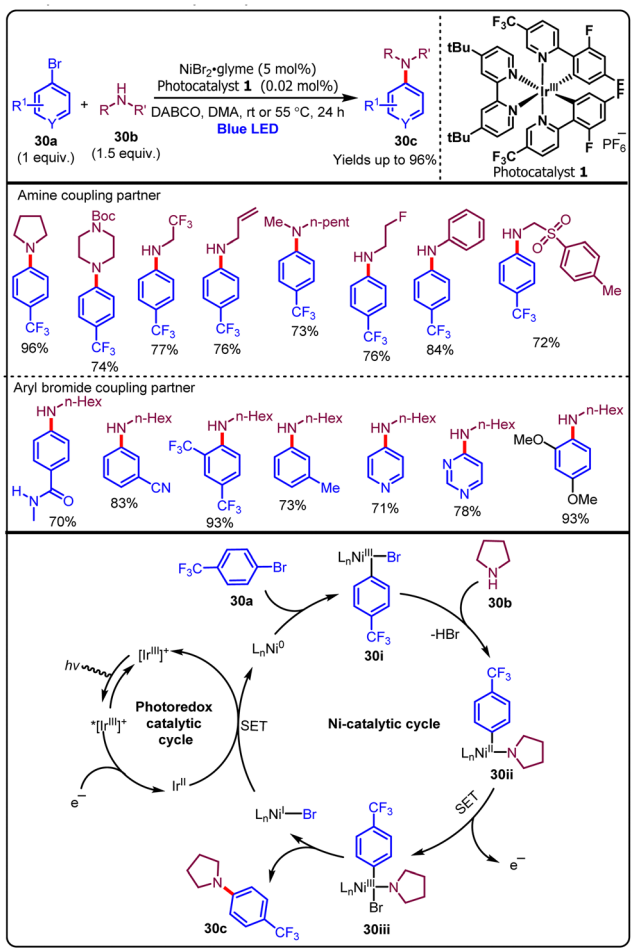

Scheme 30 Metallaphotoredox-catalyzed ligand-free redox-neutral C–N bond formation (Buchwald and MacMillan method).

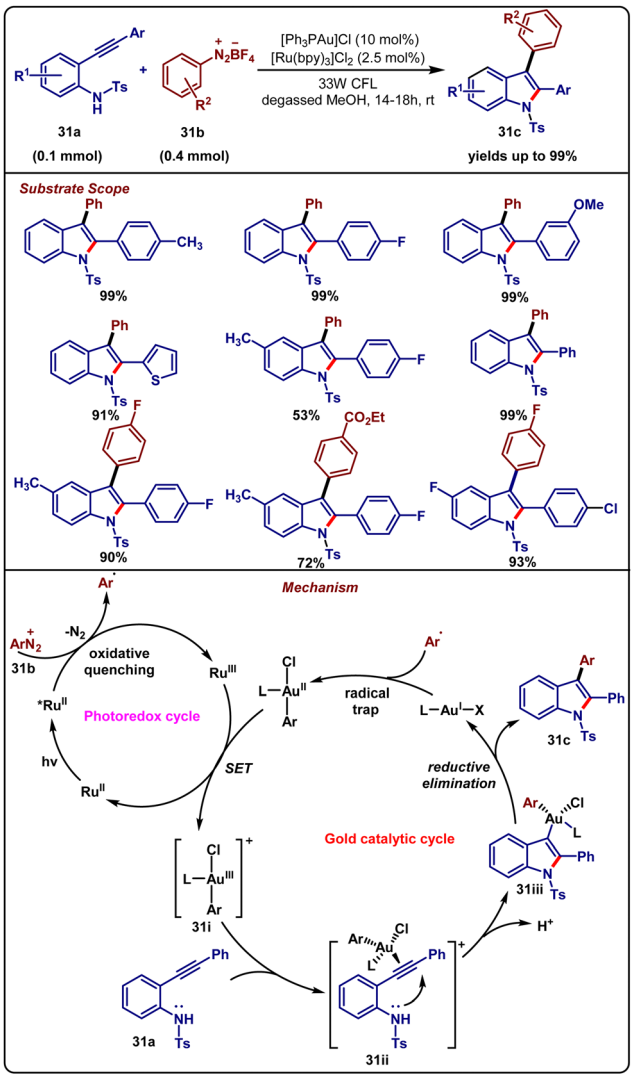

Scheme 31 Synthesis of 3-arylindoles *via* dual gold/photoredox catalysis (Zhu method).

groups on the aryl moiety performed very well under the optimized reaction conditions. Interestingly, the authors applied their reaction in flow chemistry and got an 81% yield using the same catalytic system within 15 min and obtained a 95% yield within 15 min using the $NiBr_2{\cdot}3H_2O$ catalyst. The mechanism of the reaction as proposed by the authors is shown in Scheme 30. Ir(III)-photocatalyst $Ir[dF(CF)_3ppy]_2(dtbbpy)PF_6$ initially was photoexcited to form long-lived triplet photoexcited state $*Ir^{III}$. Concomitantly, oxidative addition of bromoarene **30a** to the Ni(0)-catalyst led to the corresponding Ni(II) aryl bromide complex intermediate **30i**. Then, the generated intermediate **30i** underwent a ligand exchange reaction with amine **30b** to form the corresponding Ni(II)-aryl amido complex **30ii** along with liberation of HBr. Next, a single-electron transfer (SET) event occurred from Ni(II) complex **30ii** to the photoexcited $*Ir^{III}$ catalyst to generate Ni(III)-complex **30iii** and the reduced Ir(II) photocatalyst. Finally, the reductive elimination of the generated Ni(III) complex **30ii** yielded the Ni(I)-complex and the desired aryl aminated product **30c**. The Ni(0)-catalyst was then regenerated by the second SET with reduced Ir(II)-catalyst to complete the catalytic cycle.

In the same year, Du and Zhu *et al.*[41] reported an efficient method for the synthesis of 3-arylindoles **31c** *via* visible-light-mediated dual gold/photoredox catalysis under redox-neutral conditions (Scheme 31). On thoroughly screening the photocatalysts, it was found that $[Ru(bpy)_3]Cl_2$ afforded the highest reaction yield. The reaction showed good functional group tolerance and broad substrate scope for both *N*-Ts-2-alkynylanilines **31a** and phenyldiazonium **31b**. The most probable dual catalytic mechanistic cycle was proposed by the authors based on radical-trapping experiments. Initially, an aryl radical was generated by a photoredox reaction between visible-light activated Ru(II)* and aryl diazonium salt **31b**, which then reacted through the oxidative arylation of $[Ph_3PAuCl]$ to give an open-shell Au(II) intermediate. Thereafter, it underwent SET oxidation by Ru(III) and delivered aryl gold(III) species **31i**. Then, the coordinatively unsaturated complex **31i** activated the alkyne of the *N*-Ts-2-alkynylanilines **31a** towards nucleophilic substitution and delivered intermediate **31iii**. Finally, reductive elimination of **31iii** afforded the desired cross-coupled product **31c** and completed the gold(I)–gold(III) catalytic cycle by generating $[Ph_3PAuCl]$.

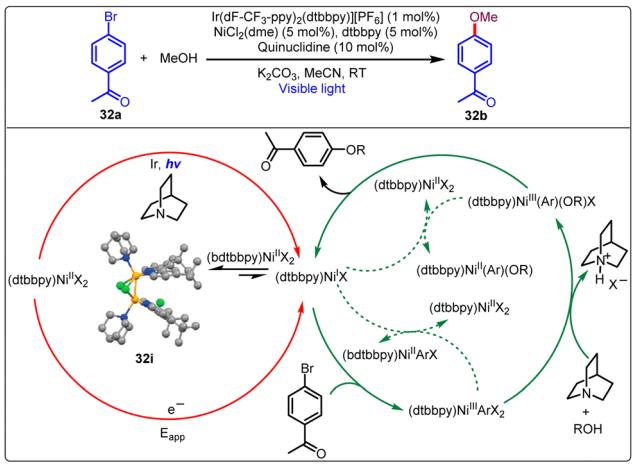

Scheme 32 Metallaphotoredox-catalyzed redox-neutral C–O bond formation (Nocera method).

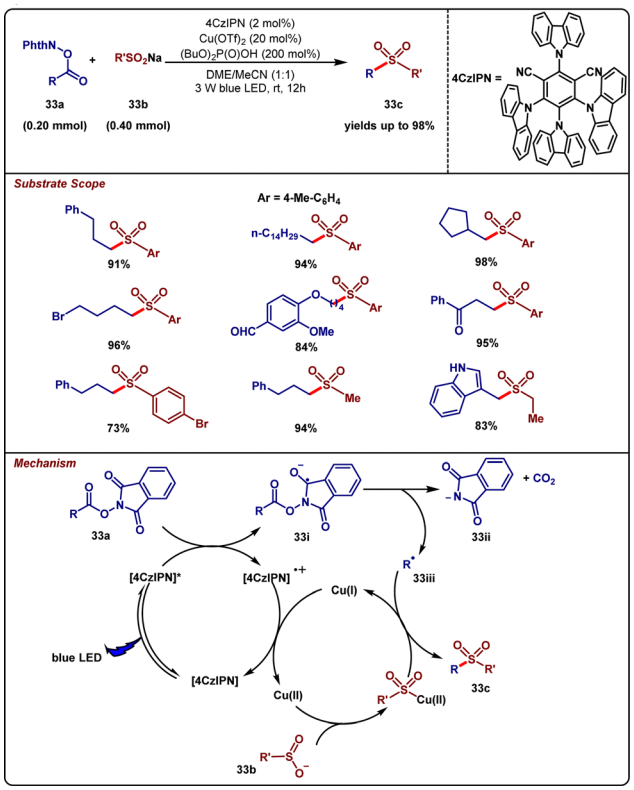

Scheme 33 Photoredox-catalyzed decarboxylative radical C(sp^3)-sulfonylation with sulfinates (Li method).

In 2019, Nocera *et al.*[42] reported a detailed mechanistic study on redox-neutral Ni-catalyzed aryl etherification under both photochemical and electrochemical conditions. According to this article, 4′-bromoacetophenone **32a** reacted with methanol in acetonitrile solvent in the presence of 1 mol% of Ir(dF-CF_3-ppy)$_2$(dtbbpy)][PF_6] as a photocatalyst, 5 mol% $NiCl_2$(dme) as a metal catalyst and dtbbpy as a ligand at room temperature under blue light irradiation (Scheme 32). 10 mol% of quinuclidine and K_2CO_3 were also required for the formation of the desired product 1-(4-methoxyphenyl)ethan-1-one **32b**. Moreover, the authors showed that this cross-coupling reaction successfully proceeded under electrochemical conditions also. Based on various experimental evidence, the authors have demonstrated that Ni-catalyzed aryl etherification involved an operative self-sustained Ni(I/III) cycle in the redox-mediated reaction under both photo- and electro-redox conditions. Additionally, the authors observed that both the quantum and faradaic yields were considerably enhanced by decreasing the photon flux and current, respectively. The putative mechanism as shown in Scheme 32 explained that the reduction of the NiX_2 precursor under photoredox conditions yielded the monomeric Ni(I) intermediate, which was trapped in solution by excess Ni(II) to form dimeric deleterious complex **32i**. The authors proposed that dissociation of the dimer was necessary for oxidative addition, after which a sustained Ni(I/III) cycle was responsible for the product formation. At high concentrations of Ni(I) or Ni(III) species, bimetallic comproportionation reactions led to inactive Ni(II) complexes and reduced the product quantum yield or Faraday efficiency.

In 2020, Liu, Li and co-workers[43] documented the redox-neutral protocol for decarboxylative radical C(sp^3)-sulfonylation with organosulfinates **33b** using photo-organocatalysis of 4CzIPN and $Cu(OTf)_2$ as a catalyst, $(BuO)_2P(O)OH$ as an additive and (1 : 1) DME and CH_3CN as the solvent mixture in the presence of blue LEDs (3 W) at room temperature. The desired sulfones **33c** were obtained in good to excellent yields within 12 h (Scheme 33). Several *N*-hydroxyphthalimide (NHPI) esters derived from primary and secondary alkyl acids underwent smooth decarboxylative sulfonylation under the optimized reaction conditions. Arenesulfinates bearing electron-withdrawing as well as electron-donating groups on the arene ring underwent sulfonylation reaction smoothly affording the desired products in good yields. Interestingly, alkanesulfinates also participated in this methodology. Based on their mechanistic studies, the authors proposed a plausible catalytic cycle for the sulfonylation reaction. The catalytic cycle began with the excitation of photocatalyst 4CzIPN generating the triplet-excited state [4CzIPN]*. A SET-type process generated NHPI ester radical anion **33i**, which underwent N–O bond cleavage to produce a carboxyl radical followed by the removal of CO_2 affording alkyl radical **33iii**. Concurrently, transmetalation of the sulfinate anion with Cu(II) formed Cu(II)–SO_2R, which was then reacted with the alkyl radical **33iii** leading to the formation the desired sulfone product **33c** and Cu(I). Finally, the Cu(I) was reoxidized by the 4CzIPN radical cation to complete the catalytic cycle.

In 2021, Nocera *et al.*[44] reported a photoredox nickel-catalyzed C–S cross-coupling reaction of aromatic halides **34a** with a variety of thiols **34b** in the presence of Ir-based photocatalyst Ir(III) (= [Ir(dF-CF_3-ppy)$_2$(dtbbpy)][PF_6], pyridine and (dme)$NiCl_2$ in acetonitrile solvent (Scheme 34). During optimization, they noticed that the addition of pyHI and a slightly elevated temperature of 55 °C were crucial for efficient C–S cross-coupling between 4-bromotoluene and thiol. Under the optimized conditions, the authors have investigated the

substrate scope with respect to aryl halides and thiols. They found that the substrate scope was restricted to aryl bromides although a variety of thiols, including aromatic as well as aliphatic thiols were well tolerated under the optimized reaction conditions (Scheme 34). The authors have done a comprehensive mechanistic study for this reaction based on time-resolved transient absorption spectroscopy, Stern–Volmer quenching, and quantum yield measurements. Based on this experimental evidence, they have (i) discovered that a self-sustained prolific Ni(I/III) cycle was responsible for quantum yield $\Phi > 1$ for the reaction; (ii) found that pyridinium iodide served as the dominant quencher for the excited state photocatalyst (*i.e.*, Ir(III)* in Scheme 34) and an important redox mediator to facilitate the formation of the active Ni(I) catalyst; and (iii) detected critical intermediates and determined the rate constants associated with their reactivity. The overall reaction pathway consisted of the following steps: (i) photoexcitation of Ir(III) to generate *Ir(III); (ii) reductive quenching of *Ir(III) by I^- to generate Ir(II) and $I^\bullet$; (iii) reduction of pyH^+ by Ir(II) to produce a pyridyl radical $pyH^\bullet$ and Ir(III); (iv) reduction of the Ni(II) pre-catalyst by $pyH^\bullet$ to give a Ni(I) species (Scheme 34); (v) oxidative addition of aryl halide to Ni(I) probably forming a Ni(III) aryl halide complex; and (vi) ligand exchange on Ni(III) and subsequent reductive elimination to release product and regenerate Ni(I). The authors further identified a minor pathway where (vii) Ni(I) was generated from the direct reaction between Ir(II) and Ni(II).

In the same year, 2021, Xiao's group[45] showcased hydroxyl-assisted dual cobalt and photoredox catalysis towards annulation of 2-propynolphenols **35a** under redox-neutral conditions. The photocatalyst of choice was 4CzIPN and $CoCl_2(PPh)_3$/5,5′-dimethyl-2,2′-bipyridine as the cobalt catalytic precursor. The propargylic alcohols bearing various substituents on the phenolic rings including electron-donating and electron-withdrawing groups such as chlorine, bromine and esters afforded the desired intramolecular cyclization product **35b**. This method could be applied for gram-scale synthesis and derivatization of pharmaceutically active molecules. The authors proposed a mechanism based on several control experiments, including radical capture using TEMPO and light on/off experiments. Initially, the photosensitizer 4CzIPN was irradiated by blue LEDs to its excited state 4CzIPN*. Herein, the authors proposed two probable pathways for the reduction of Co(II) to

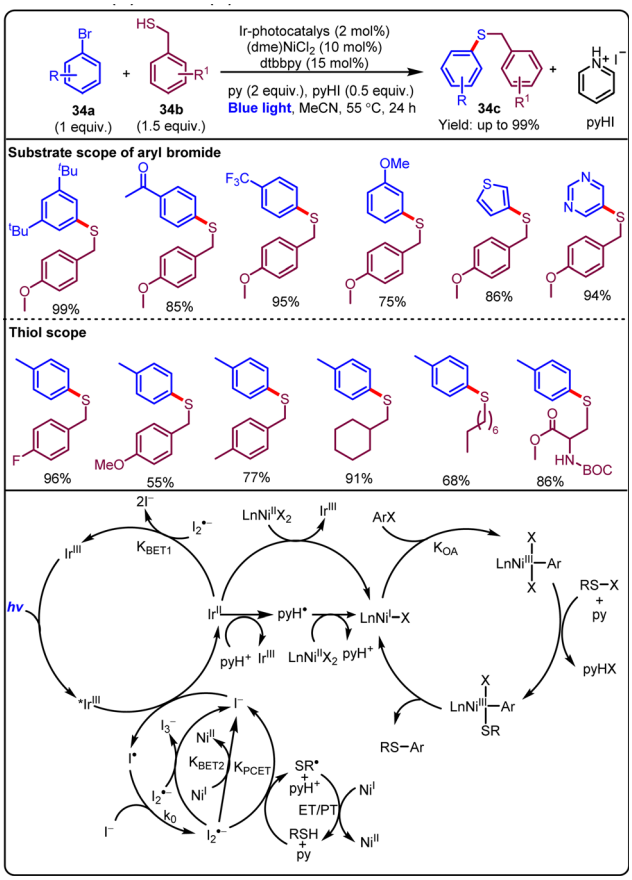

Scheme 34 Metallaphotoredox-catalyzed redox-neutral aryl thiolation, Ni^{II} = $LnNi^{II}X_2$; Ni^I = $LnNi^IX$; ET = electron transfer; and PT = proton transfer (Nocera method).

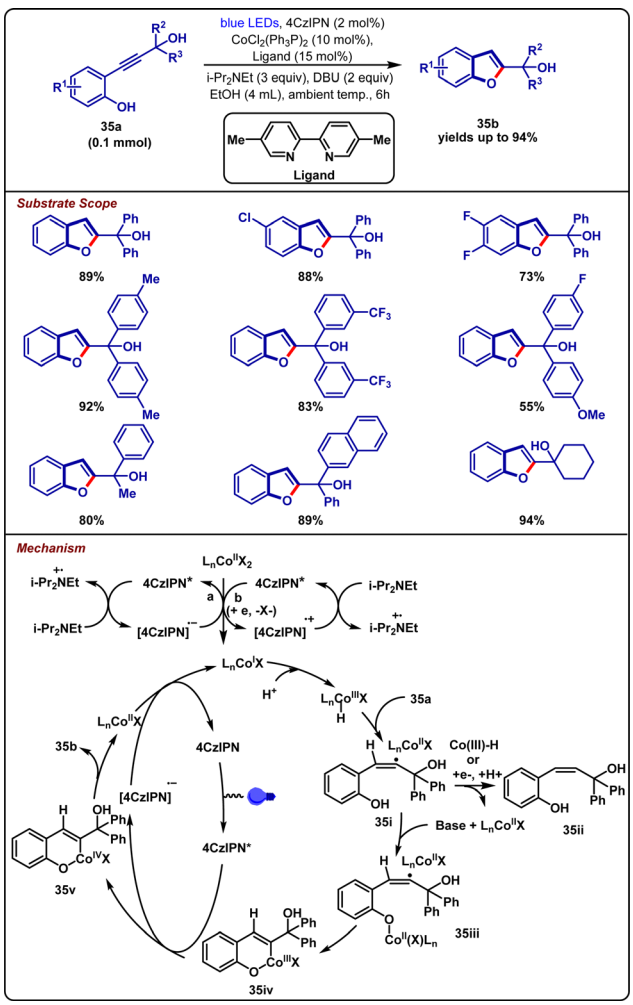

Scheme 35 Dual cobalt and photoredox-catalyzed annulation of 2-propynolphenols under redox-neutral conditions (Xiao mathod).

Co(I). In path a, quenching of photoexcited 4CzIPN* by i-Pr_2NEt afforded the [4CzIPN] radical anion and radical cation of i-Pr_2NEt followed by one-electron reduction of the Co(II)-complex by $[4CzIPN]^{\bullet-}$ to Co(I) species and regeneration of the catalyst 4CzIPN. In pathway b, the oxidative quenching of 4CzIPN* by Co(II) furnished the oxidative photosensitizer 4CzIPN radical cation. Then, the generated Co(I)-species was trapped by H^+ to give the Co(III)–H species, which subsequently underwent HAT reaction with **35a** producing radical cage intermediate **35i**. Intermediate **35i** could react with Co(III)–H or an electron and proton and furnished by-product **35ii**. In the main catalytic cycle, substitution occurred with the phenolic hydroxyl group of intermediate **35i** and the cobalt center in the presence of base and generated intermediate **35iii**, which would convert to six-membered cyclic intermediate **35iv** *via* Co–C bond formation. Intermediate **35iv** subsequently underwent SET oxidation by 4CzIPN* giving Co(IV)-intermediate **35v**. Finally, reductive elimination of **35v** offered the desired product **35b** and Co(II) followed by reduction with the 4CzIPN radical anion to regenerate the Co(I)-catalyst to complete the catalytic cycle (Scheme 35).

7. Conclusions

In conclusion, this article summarizes the recent advancements in redox-neutral C–X bond formation reactions based on active intermediate(s) involved under photoredox catalysis, which have been published up until March, 2023. Due to the broad range of industrial and pharmaceutical importance of the products, C–X coupling reaction has been booming rapidly and greater numbers of articles have been published recently. The literature results indicated that the excited state redox potential of the photocatalyst has a significant impact on the rate of the reaction. To initiate the reaction, quenching pathways (either oxidative or reductive) were the main ones for photoredox catalysis. The effect of the light source, solvent, base, and additives also have significant roles in efficiently converting reactants to products.

In spite of the rapid progress in this photochemical strategy, a few challenges still remain that need to be addressed. There is a lack of progress in developing either earth-abundant first row transition-metal-based photoredox catalysts or organo-photoredox catalysts for this redox-neutral C–X coupling reaction. The use of an additional catalytic cycle (involvement of additional metal) is also required in some photocatalytic systems. Therefore, the development of new and efficient photochemical methodologies on the proposed topic is fascinating as well as challenging. In this scenario, the application of organic photosensitizers could also be effective, which can avoid metal-contamination. The use of modern technologies, such as batch reactor, micro reactor technologies and continuous flow processes can be a solution for long reaction times. The use of sunlight can give more efficiency. Moreover, the mechanistic studies should be carefully evaluated as appropriate knowledge of the mechanism can lead to the development of new methodologies. Finally, we hope that this review article will attract more readers among synthetic organic chemists who will carry out more research to dig deep inside the topic.

Conflicts of interest

There are no conflicts to declare.

Acknowledgements

A. H. acknowledges financial support from SERB, New Delhi (grant no. CRG/2020/000362).

Notes and references

1 K. C. Nicolaou, *Proc. R. Soc. A*, 2014, **470**, 20130690.
2 (*a*) C. Sambiagio and T. Noël, *Trends Chem.*, 2020, **2**, 92–106; (*b*) R. C. McAtee, E. J. McClain and C. R. J. Stephenson, *Trends Chem.*, 2019, **1**, 111–125; (*c*) B. M. Hockin, C. Li, N. Robertson and E. Zysman-Colman, *Catal. Sci. Technol.*, 2019, **9**, 889–915; (*d*) F. Guba, Ü. Tastan, K. Gugeler, M. Buntrock, T. Rommel and D. Ziegenbalg, *Chem. Ing. Tech.*, 2019, **91**, 17–29; (*e*) D. Cambié, C. Bottecchia, N. J. W. Straathof, V. Hessel and T. Noël, *Chem. Rev.*, 2016, **116**, 10276–10341; (*f*) Q.-Q. Zhou, Y.-Q. Zou, L.-Q. Lu and W.-J. Xiao, *Angew. Chem., Int. Ed.*, 2019, **58**, 1586–1604; (*g*) C. K. Prier, D. A. Rankic and D. W. C. MacMillan, *Chem. Rev.*, 2013, **113**, 5322–5363; (*h*) D. W. C. MacMillan, *Nature*, 2008, **455**, 304–308; (*i*) D. A. Nicewicz and D. W. C. MacMillan, *Science*, 2008, **322**, 77–80; (*j*) M. H. Shaw, J. Twilton and D. W. C. MacMillan, *J. Org. Chem.*, 2016, **81**, 6898–6926; (*k*) J. Twilton, C. Le, P. Zhang, M. H. Shaw, R. W. Evans and D. W. C. MacMillan, *Nat. Rev. Chem.*, 2017, **1**, 0052; (*l*) C. R. J. Stephenson, T. P. Yoon and D. W. C. MacMillan, *Visible Light Photocatalysis in Organic Chemistry*, Wiley-VCH, 2018; (*m*) Y. Tan, J. M. Muñoz-Molina, G. C. Fu and J. C. Peters, *Chem. Sci.*, 2014, **5**, 2831–2835; (*n*) N. A. Romero and D. A. Nicewicz, *Chem. Rev.*, 2016, **116**, 10075–10166.
3 B. König, *Eur. J. Org. Chem.*, 2017, 1979–1981.
4 (*a*) A. J. Waldman, T. L. Ng, P. Wang and E. P. Balskus, *Chem. Rev.*, 2017, **117**, 5784–5863; (*b*) A. Gomtsyan, *Chem. Heterocycl. Compd.*, 2012, **48**, 7–10; (*c*) Y.-J. Wu, in *Progress in Heterocyclic Chemistry*, ed. G. W. Gribble and J. A. Joule, Elsevier, 2012, vol. 24, pp. 1–53; (*d*) P. N. Kalaria, S. C. Karad and D. K. Raval, *Eur. J. Med. Chem.*, 2018, **158**, 917–936.
5 (*a*) B. C. Ranu, T. Chatterjee and N. Mukherjee, in *Ball Milling Towards Green Synthesis: Applications, Projects, Challenges*, The Royal Society of Chemistry, 2015, pp. 1–33, DOI: **10.1039/9781782621980-00001**; (*b*) J. Bariwal and E. Van der Eycken, *Chem. Soc. Rev.*, 2013, **42**, 9283–9303; (*c*) A. Bhunia, S. R. Yetra and A. T. Biju, *Chem. Soc. Rev.*, 2012, **41**, 3140–3152; (*d*) B. Banerjee, *Curr. Microwave Chem.*, 2020, **7**, 84–85; (*e*) S. Ghosh, D. Lai and A. Hajra, *Org. Biomol. Chem.*, 2021, **19**, 2399–2415; (*f*) S. Ghosh, D. Ghosh and A. Hajra, *Phys. Sci. Rev.*, 2021, **7**, 215–235; (*g*) Z. Zeng, A. Feceu, N. Sivendran and L. J. Gooßen, *Adv. Synth. Catal.*, 2021, **363**, 2678–2722; (*h*) A. Sarkar, S. Santra, S. K. Kundu, A. Hajra, G. V. Zyryanov, O. N. Chupakhin, V. N. Charushin and A. Majee, *Green Chem.*, 2016, **18**, 4475–4525; (*i*) C. Cavedon, P. H. Seeberger and B. Pieber, *Eur. J. Org. Chem.*, 2020, 1379–1392; (*j*) S. Ghosh, S. Mondal and A. Hajra, *Adv. Synth. Catal.*, 2020, **362**, 3768–3794; (*k*) D. Ghosh, S. Ghosh and A. Hajra, *Adv. Synth. Catal.*, 2021, **363**, 5047–5071; (*l*) J. Das, T. Pal, W. Ali, S. R. Sahoo and D. Maiti, *ACS Catal.*, 2022, **12**, 11169–11176; (*m*) S. K. Sinha, S. Panja, J. Grover, P. S. Hazra, S. Pandit, Y. Bairagi, X. Zhang and D. Maiti, *J. Am. Chem. Soc.*, 2022, **144**, 12032–12042; (*n*) Y. Wei, I. Deb and N. Yoshikai, *J. Am. Chem. Soc.*, 2012, **134**, 9098–9101.
6 (*a*) D. Das, A. X. Sun and D. Seidel, *Angew. Chem., Int. Ed.*, 2013, **52**, 3765–3769; (*b*) D. Zhao, Z. Shi and F. Glorius, *Angew. Chem., Int. Ed.*, 2013, **52**, 12426–12429; (*c*) W. Chen, Y. Kang, R. G. Wilde and D. Seidel, *Angew. Chem., Int. Ed.*, 2014, **53**, 5179–5182; (*d*) Q. Zhao and M. Szostak, *ChemSusChem*, 2019, **12**, 2983–2987; (*e*) Q. Wu,

D. Yan, Y. Chen, T. Wang, F. Xiong, W. Wei, Y. Lu, W.-Y. Sun, J. J. Li and J. Zhao, *Nat. Commun.*, 2017, **8**, 14227; (*f*) M. T. Richers, M. Breugst, A. Y. Platonova, A. Ullrich, A. Dieckmann, K. N. Houk and D. Seidel, *J. Am. Chem. Soc.*, 2014, **136**, 6123–6135; (*g*) Z. Zhang, L.-L. Liao, S.-S. Yan, L. Wang, Y.-Q. He, J.-H. Ye, J. Li, Y.-G. Zhi and D.-G. Yu, *Angew. Chem., Int. Ed.*, 2016, **55**, 7068–7072.
7 H. Wang and H. Huang, *Chem. Rec.*, 2016, **16**, 1807–1818.
8 J. Xie, H. Jin and A. S. K. Hashmi, *Chem. Soc. Rev.*, 2017, **46**, 5193–5203.
9 D. Ghosh, S. Ghosh, A. Ghosh, P. Pyne, S. Majumder and A. Hajra, *Chem. Commun.*, 2022, **58**, 4435–4455.
10 (*a*) S. Neogi, A. K. Ghosh, S. Mandal, D. Ghosh, S. Ghosh and A. Hajra, *Org. Lett.*, 2021, **23**, 6510–6514; (*b*) A. K. Bagdi, M. Rahman, D. Bhattacherjee, G. V. Zyryanov, S. Ghosh, O. N. Chupakhin and A. Hajra, *Green Chem.*, 2020, **22**, 6632–6681; (*c*) G. Kibriya, D. Ghosh and A. Hajra, *Sci. China: Chem.*, 2020, **63**, 42–46; (*d*) G. Kibriya, S. Mondal and A. Hajra, *Org. Lett.*, 2018, **20**, 7740–7743; (*e*) M. Singsardar, A. Dey, R. Sarkar and A. Hajra, *J. Org. Chem.*, 2018, **83**, 12694–12701; (*f*) G. Kibriya, S. Samanta, S. Jana, S. Mondal and A. Hajra, *J. Org. Chem.*, 2017, **82**, 13722–13727.
11 A. J. Musacchio, L. Q. Nguyen, G. H. Beard and R. R. Knowles, *J. Am. Chem. Soc.*, 2014, **136**, 12217–12220.
12 H. Jiang and A. Studer, *Angew. Chem., Int. Ed.*, 2017, **56**, 12273–12276.
13 L. Wang, P. Cheng, X. Wang, W. Wang, J. Zeng, Y. Liang and O. Reiser, *Org. Chem. Front.*, 2019, **6**, 3771–3775.
14 Q. Fu, Z.-Y. Bo, J.-H. Ye, T. Ju, H. Huang, L.-L. Liao and D.-G. Yu, *Nat. Commun.*, 2019, **10**, 3592.
15 J.-L. Tu, W. Tang and F. Liu, *Org. Chem. Front.*, 2021, **8**, 3712–3717.
16 (*a*) J. Wang, M. Sánchez-Roselló, J. L. Aceña, C. del Pozo, A. E. Sorochinsky, S. Fustero, V. A. Soloshonok and H. Liu, *Chem. Rev.*, 2014, **114**, 2432–2506; (*b*) X. Zhang and S. Cao, *Tetrahedron Lett.*, 2017, **58**, 375–392.
17 Q.-S. Gao, Z. Niu, Y. Chen, J. Sun, W.-Y. Han, J.-Y. Wang, M. Yu and M.-D. Zhou, *Org. Lett.*, 2021, **23**, 6153–6157.
18 M. Zhang, X. Ding, A. Lu, J. Kang, Y. Gao, Z. Wang, H. Li and Q. Wang, *Org. Chem. Front.*, 2021, **8**, 961–967.
19 Z.-T. Luo, J.-H. Fan, B.-Q. Xiong, Y. Liu, K.-W. Tang and P.-F. Huang, *Eur. J. Org. Chem.*, 2022, e202200793.
20 B. Wang, M.-J. Zhou and Q.-L. Zhou, *Org. Lett.*, 2022, **24**, 2894–2898.
21 Q.-C. Gan, J. Qiao, C. Zhou, R.-N. Ci, J.-D. Guo, B. Chen, C.-H. Tung and L.-Z. Wu, *Angew. Chem., Int. Ed.*, 2023, **62**, e202218391.
22 M. Zhang, J. Zhang and M. Oestreich, *Nat. Synth.*, 2023, DOI: 10.1038/s44160-023-00256-z.
23 S. Ventre, F. R. Petronijevic and D. W. C. MacMillan, *J. Am. Chem. Soc.*, 2015, **137**, 5654–5657.
24 L. Candish, L. Pitzer, A. Gómez-Suárez and F. Glorius, *Chem. – Eur. J.*, 2016, **22**, 4753–4756.
25 W. Shu, E. Merino and C. Nevado, *ACS Catal.*, 2018, **8**, 6401–6406.
26 T. M. Monos, R. C. McAtee and C. R. J. Stephenson, *Science*, 2018, **361**, 1369–1373.
27 C. Huang, J. Feng, R. Ma, S. Fang, T. Lu, W. Tang, D. Du and J. Gao, *Org. Lett.*, 2019, **21**, 9688–9692.
28 Z.-H. Luan, J.-P. Qu and Y.-B. Kang, *J. Am. Chem. Soc.*, 2020, **142**, 20942–20947.
29 E. W. Webb, J. B. Park, E. L. Cole, D. J. Donnelly, S. J. Bonacorsi, W. R. Ewing and A. G. Doyle, *J. Am. Chem. Soc.*, 2020, **142**, 9493–9500.
30 M. M. D. Pramanik, F. Yuan, D.-M. Yan, W.-J. Xiao and J.-R. Chen, *Org. Lett.*, 2020, **22**, 2639–2644.
31 M.-S. Liu and W. Shu, *ACS Catal.*, 2020, **10**, 12960–12966.
32 P. J. Sarver, N. B. Bissonnette and D. W. C. MacMillan, *J. Am. Chem. Soc.*, 2021, **143**, 9737–9743.
33 L. Ge, C. Zhang, C. Pan, D.-X. Wang, D.-Y. Liu, Z.-Q. Li, P. Shen, L. Tian and C. Feng, *Nat. Commun.*, 2022, **13**, 5938.
34 C. Zhou, T. Lei, X.-Z. Wei, C. Ye, Z. Liu, B. Chen, C.-H. Tung and L.-Z. Wu, *J. Am. Chem. Soc.*, 2020, **142**, 16805–16813.
35 V. A. Pistritto, S. Liu and D. A. Nicewicz, *J. Am. Chem. Soc.*, 2022, **144**, 15118–15131.
36 K. Luo, Y. Zhao, Z. Tang, W. Li, J. Lin and Y. Jin, *Org. Lett.*, 2022, **24**, 6335–6340.
37 A. Y. Chan, I. B. Perry, N. B. Bissonnette, B. F. Buksh, G. A. Edwards, L. I. Frye, O. L. Garry, M. N. Lavagnino, B. X. Li, Y. Liang, E. Mao, A. Millet, J. V. Oakley, N. L. Reed, H. A. Sakai, C. P. Seath and D. W. C. MacMillan, *Chem. Rev.*, 2022, **122**, 1485–1542.
38 J. A. Terrett, J. D. Cuthbertson, V. W. Shurtleff and D. W. C. MacMillan, *Nature*, 2015, **524**, 330–334.
39 J. Xuan, T.-T. Zeng, J.-R. Chen, L.-Q. Lu and W.-J. Xiao, *Chem. – Eur. J.*, 2015, **21**, 4962–4965.
40 E. B. Corcoran, M. T. Pirnot, S. Lin, S. D. Dreher, D. A. DiRocco, I. W. Davies, S. L. Buchwald and D. W. C. MacMillan, *Science*, 2016, **353**, 279–283.
41 C. Qu, S. Zhang, H. Du and C. Zhu, *Chem. Commun.*, 2016, **52**, 14400–14403.
42 R. Sun, Y. Qin, S. Ruccolo, C. Schnedermann, C. Costentin and D. G. Nocera, *J. Am. Chem. Soc.*, 2019, **141**, 89–93.
43 J. He, G. Chen, B. Zhang, Y. Li, J.-R. Chen, W.-J. Xiao, F. Liu and C. Li, *Chem*, 2020, **6**, 1149–1159.
44 Y. Qin, R. Sun, N. P. Gianoulis and D. G. Nocera, *J. Am. Chem. Soc.*, 2021, **143**, 2005–2015.
45 Y. Zhu, Y.-Q. He, W.-F. Tian, M. Wang, Z.-Z. Zhou, X.-R. Song, H.-X. Ding and Q. Xiao, *Adv. Synth. Catal.*, 2021, **363**, 3372–3377.